Studying the Role of Modified Aptamer-8 for Efficient Detection of Immunoglobin-G Antibodies

By

Tehmina Azam

School of Chemical and Materials Engineering

National University of Sciences and Technology

2023

Studying the Role of Modified Aptamer-8 for Efficient Detection of Immunoglobin-G Antibodies.

Tehmina Azam

Reg.No:00000328135

This thesis is submitted as a partial fulfillment of the requirements for the degree of

"Master of Science (MS) in Nanoscience and Engineering"

Supervisor Name: Dr. Usman Liaqat

School of Chemical and Materials Engineering (SCME)

National University of Sciences and Technology (NUST)

H-12 Islamabad, Pakistan

May, 2023

"In the name of Allah Almighty, The Most Gracious, The Most Merciful"

Dedication

To my own dedication and hard work, without which this thesis would not have been possible, and to my family, who provided unwavering support and encouragement.

Acknowledgments

I would like to express my deepest gratitude to all those who have supported me throughout my academic journey and the completion of this thesis. Primarily, I would like to acknowledge my own devotion and hard work in bringing this project to fruition. The countless hours spent in the lab, conducting experiments, analyzing data, and writing have been challenging but incredibly rewarding.

I would also like to thank my supervisor Dr. Usman Liaqat for providing invaluable guidance and support throughout the project. The expertise, patience, and encouragement of my co-supervisor and GEC members have been instrumental in shaping the direction of this work and pushing me to achieve my full potential.

I would like to extend my acknowledgements to my family, whose untiring support and love have been a constant source of inspiration and motivation. Their encouragement and understanding throughout my academic journey have been instrumental in my success.

Finally, I would like to express my gratitude to my lab fellows, friends and colleagues for their encouragement, helpful discussions, and support throughout this project. Their input and feedback have been influential in shaping the direction of this work and contributing to its success.

-Tehmina Azam

Abstract

Immunoglobulin G (IgG) plays a critical role in the diagnosis of multiple pathological conditions, including autoimmune hepatitis, hepatitis B virus (HBV), chickenpox, and MMR (Mumps, Measles, and Rubella). However, dependable, sensitive, and selective IgG detection remains a challenge. The recent outbreak of SARS-CoV-2 has highlighted the significance of IgG biosensing. Therefore, this study aims to develop a novel IgG biosensing platform with improved reliability, sensitivity, and selectivity. The proposed biosensing platform consists of Aptamer 8 as a biorecognition element and gold interdigitated electrodes (IDEs) modified with perfluoro decanethiol (PFDT) as its main constituents. The IDEs were immersed in the PFDT solution for the self-assembled monolayer (SAM) deposition process for 24 hours at room temperature (RT), and then dried in a glove box with a nitrogen atmosphere. Aptamer 8 was used to functionalize PFDT-IDEs, and several dilutions of IgG were incubated onto the biosensor for the detection studies. Contact angle, SEM, AFM, XRD, FTIR spectroscopy, and electrochemical studies were done for characterization and detection studies. The proposed biosensing platform showed a limit of detection (LOD) of 13 ug/ml. Characterization studies demonstrated the successful modification of PFDT on IDEs and the functionalization of Aptamer 8 on PFDT-IDEs. Electrochemical studies revealed a significant increase in the current response upon the incubation of IgG on the biosensor. The proposed IgG biosensing platform with Aptamer 8 and gold interdigitated electrodes modified with perfluoro decanethiol showed improved reliability, sensitivity, and selectivity. This biosensing platform has potential applications for high throughput systems and point-of-care detection of IgG and other biomolecules. Future studies should focus on optimizing the biosensor's performance and exploring its application in clinical settings.

Contents

List of Figures

List of Tables

List of Abbreviations

IgG	Immunoglobulin G
SARS-CoV-2	Severe Acute Respiratory Syndrome Coronavirus 2.
HBV	Hepatitis B Virus
MMR	Measles, Mumps, and Rubella
IDEs	Interdigitated Electrodes
PFDT	Perfluoro decanethiol
SAM	Self-Assembled Monolayer
RT	Room Temperature
RNA	Ribonucleic Acid
DNA	Deoxyribonucleic Acid
CMP	Carboxymethyl pullulan
CHI	Chitosan
D.I water	Deionized water
XRD	X-ray Diffraction
SEM	Scanning Electron Microscopy
FTIR	Fourier Transform Infra-Red
EDS	Energy Dispersive X-ray spectroscopy

Chapter: 1

Introduction

1.1 Background to Biosensing

In the healthcare sector, diagnosis or identification is an important term that refers to the investigation of a disease before planning the treatment strategy [1]. Molecules including enzymes, antibodies, antigens, proteins, ribonucleic acid (RNA), and deoxyribonucleic acid (DNA) play a pivotal role in controlling the basic cellular cycles hence they are considered an important biological marker [2]. The association of these biomarkers with various normal and abnormal phenomena accruing in the human body demands their quick and accurate identification methods. For this specific purpose, a substantial number of tests have been reported in research articles and some are being practiced in laboratories [3, 4]. In this regard, small devices known as biosensors are of immense importance as they help in the speedy and accurate detection of biological analytes (biomarkers) [5-7]. These advancements in point-of-care devices have helped the diagnostic area to pave its way in both clinical laboratories and research divisions of the healthcare sector. Despite all these improvements, the sensitivity, selectivity, accuracy, and swiftness of biosensors are still major challenges, but nanotechnology has shown its perks to tackle the hurdles [8-10]. The use of nanomaterials has given extraordinary characteristics to diagnostic kits (biosensors) hence improving the limit of detection, efficiency, selectivity, and cost effectivity biosensors. The importance of nanomaterials from nanoparticles to nanocomposites cannot be denied as they are intelligently being used in healthcare areas the food industry to textile mills and many more [11].

1.2 Introduction to Biosensing

A device that helps in the identification and quantification of biological or chemical reactions is known as a biosensor. The use of electronic principles in biology and medicine is the subject of bioelectronics. A unique kind of bioelectronic tool frequently employed in bioanalysis is the biosensor. The "primary element of a measurement chain, which converts the input variable into a signal suitable for measurement" might be thought of as a sensor. The techniques and materials

required to construct biosensing actuators have been made available to us thanks to numerous significant technical advancements during the past ten years. The sensitivity, discrimination, and multiplexing potentials of current biosensing devices have significantly improved since the creation of the Clark oxygen electrode sensor [12]. A biosensor is an independent receptor transducer device that may provide specific measurable or semiquantitative investigative information employing a biological identification element, according to IUPAC standards from 1999 [13].

The reactions are measured with the help of small signals produced during the process of measurement. These signals are made visible in the form of changes in the color, voltage, current, resistance, or conductivity of the device[14]. The substance which is analyzed or measured by biosensors is known as an analyte [15]. Various analytes are required to be identified in small proportions. These molecules include proteins, antibodies, antigens, enzymes, RNA and DNA. A biosensor's signals are always inversely correlated with the concentration of the analytes being monitored [16]. Applications for biosensors include disorder examining, drug development, and the recognition of toxins, disease-causing microorganisms, and ailment indicators in bodily fluids (blood, urine, saliva, sweat) [17].

A biosensor's main function is to deliver the interrogating analyte with quick, real-time, precise, and dependable data. The ideal instrument is one that can react continuously, reversibly, and without disturbing the sample. Apart from that in medicine, agriculture, food security, bioprocessing, and ecological and industrial monitoring, biosensors have been anticipated to participate a key analytical role [18].

To monitor the concentration of glucose directly, Clark and Lyons connected glucose oxidase to an amperometric oxygen electrode surface in 1962, creating the first biosensor. By incorporating "enzyme transducers as membrane-enclosed sandwiches," they explained how to "make electrochemical sensors (pH, polarographic, potentiometric, or conductometric) more intelligent" [19].

1.3 Components of a Typical Biosensor

Looking into the technological aspect, a biosensor is miniaturized device which has an integrated layer consisting of biorecognition element which is connected to a transduction platform for signal generation. The bio-sensitive layer can be formed using one of many biomolecules (enzymes, receptors, antibodies, whole cells,

antigens, microbes, and oligonucleotides) on the biosensors surface. The use these biomolecules make a bio sensitive layer more sensitive and specific to an analyte (toxins, viruses or their proteins, RNA/DNA etc.) and this binding event leads to the signals generation [20].

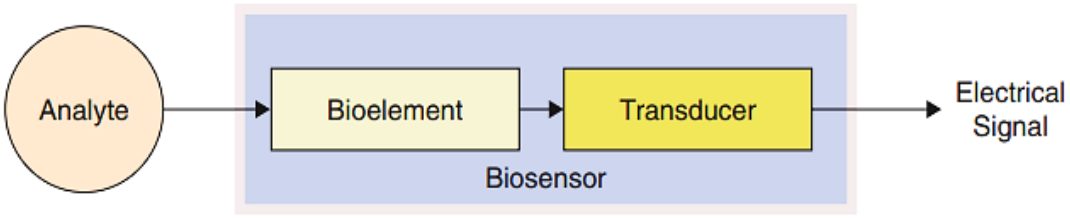

Figure 1: Working principle of a typical biosensor. It shows the three important components of a biosensor i.e., biorecognition element, transducer, and signal processing components.

If mentioned in details an analyte, bioreceptor, transducer, electronics and display are main components of a bioreceptor as initially introduced above [21].

- **Analyte**: An analyte is a target substance that needs to be located or recognized in a sample. An example of an "analyte" is glucose, which is used in the detection of glucose.
- **Bioreceptor**: The bioreceptor or biorecognition helps in the specific identification of biological molecules and bioreceptors including aptamers, enzymes, oligonucleotides, proteins, and antibodies. Bioreceptors works on the principle of biorecognition which refers to the signal generation in the form of current, voltage, resistance, and capacitance due to the interaction between two biomolecules.
- **Transducer**: An element referred to as a transducer converts one form of energy into another. The bio-recognition event and a quantifiable signal are connected via the transducer in a biosensor. This process of power shift is known as signalization. Most transducers create electrical or optical signals, which are typically proportionate to the quantity of interactions between analyte and bioreceptor.
- **Electronics**: The transduced signal is processed and prepared for display in this region of a biosensor. It is composed of complex electronic circuitry that conducts signal conditioning tasks including amplifying and converting analog

signals into digital ones. The biosensor's display unit then quantifies the processed signals.

- **Display**: The specific data of a user interpretation system is created in numbers or curves that the user can comprehend, like the liquid crystal display on a computer or the printhead of an important printer. This element often consists of a mix of hardware and software to produce data from the biosensor that is easy to understand. The output signal on the display can be numerical, graphic, tabular, or even an image, depending on the demands of the end user.

1.4 Types of Biosensors

Biosensors can be classified based on their process or working principle. One common classification scheme is based on the type of transducer used to convert the biological recognition event into a measurable signal. Examples of transducer types include optical biosensors, electrochemical biosensors, piezoelectric biosensors, and thermal biosensors. Optical biosensors use light as the transducer, while electrochemical biosensors use electrical signals. Piezoelectric biosensors use a crystal that changes shape when it binds to a target molecule, generating an electrical signal. Thermal biosensors detect changes in temperature caused by a biological reaction. Another way to classify biosensors is based on the type of biorecognition element. Some common types include enzymatic biosensors, immunosensors, nucleic acid biosensors, microbial biosensors, whole-cell biosensors, and aptamer-based biosensors. Enzymatic biosensors use enzymes as the biological recognition element, while immunosensors use antibodies to detect specific antigens or proteins. Nucleic acid biosensors use DNA or RNA as the recognition element, and microbial biosensors use microorganisms to detect and quantify analytes. Whole-cell biosensors use living cells to detect and respond to environmental changes. Aptamer-based biosensors use aptamers, which are short, single-stranded DNA or RNA molecules that can specifically bind to target molecules. All types are compiled in the table given below [22].

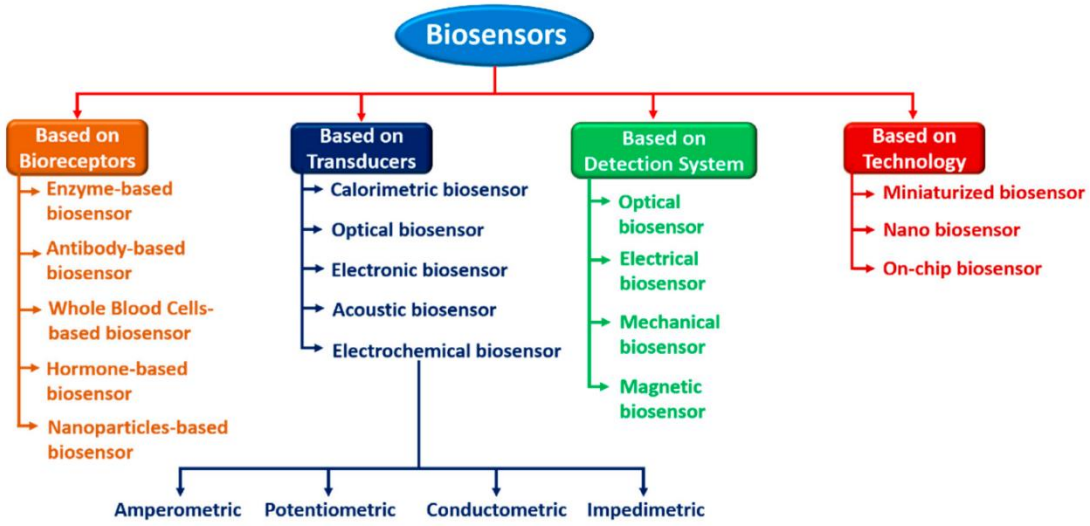

Figure 2: Types of biosensors. Biosensors are classified based on biorecognition element and transduction mechanism used as the working principle of a biosensor.

1.4.1 Enzymatic Biosensor

An analytical tool with an enzyme acting as a bioreceptor that is integrated into or intricately linked to the physical transducer is known as an "enzymatic biosensor." These devices generate discrete or continuous digital electronic/optical signals that are proportional to the concentration of analytes present in the sample [23]. Using a Clark oxygen electrode, glucose oxidase can be incorporated in the proximity to electrode while the oxygen level is being tracked. When a platinum WE (working electrode) is utilized, the generated hydrogen peroxide can be detected in the form of current at a potential of roughly about +0.7 V vs Ag/AgCl [12]. Apart from that another biosensor was proposed for the detection of urea which also works due to the urease enzyme for monitoring its analyte concentration in aqueous solutions for biological applications. Two different strategies were used in this study including physisorption of enzyme and layer by layer film deposition atop an electrodeposited polyaniline film (PANI). Charged polysaccharides were alternately deposited to create the LbL. The potentiometric responses of the enzymatic biosensors were assessed in relation to the urea content in aqueous solutions. (Ranging from 106 to 101 mol L1 urea). Extremely high sensitivity and a quick response time were observed for the current biosensor [24].

1.4.2 Antibody Biosensor

The immune system fights off infectious pathogens that can be detrimental to the host to protect the body. Its two primary subcategories are non-adaptive (innate)

immunity and acquired (adaptive) immunity. The first one refers to broad protection processes that start working hours or even minutes after an antigen enters the body. These immune responses rely on physical defences like the skin as well as groups of proteins and protective cells like neutrophils, monocytes, macrophages, mast cells, and dendritic cells that quickly activate upon identifying specific characteristics of foreign molecules and remove or eradicate the alien species. On the other hand, the second type of immune system is highly specific to a single disease. Compared to acquired immune responses, innate immune responses are easier. The antigen must first be identified and processed. Specifically, the immune system generates a swarm of immune cells designed specifically to fight an antigen after it has been discovered. The secretion of immunoglobulins by lymphocytes controls the development of acquired immunity. (Igs). The best thing about acquired immunity is that it creates immunological memory after first encounter to a specific pathogen, leading to an enhanced response to that disease in future combats [25].

1.4.3 DNA Based Biosensors

The expansion of DNA-based biosensors has accelerated over the last 20 years. Numerous devices of DNA detection platforms have been suggested to respond to diverse molecular indicators, including oligonucleotides, amino acids, lipids, tiny ions, and other molecules involved in biological processes. Their usage has been made easier by contemporary nanotechnology, groundbreaking enzyme engineering, excellent designs based on intricate sequence programs, exact base changes, and in vivo and in vitro uses of DNA-based biosensors. In recent years, numerous well-known DNA-based sensing platforms have been described and are now widely employed in a range of fields, such as environmental monitoring, food security, clinical diagnostics, disease prognosis, etc. [26].

DNA is a promising candidate for intelligent biosensing due to its remarkable addressability, more long-lasting biological activity, and adjustable rigidity when compared to commonly used bio probes. According to reports, DNA probes like aptamers can be manually screened and modified to improve their thermal stability. Varying biological affinity and increased protection against enzymatic attack. Additionally, DNA could be used as a template to create programmable macromolecule configurations that allow for precise control over the spatial position of alterations. This may enhance the performance of the biosensor and might

encourage scientists to suggest new biosensor designs [27-30]. The most popular method for using a DNA aptamer to detect a biotarget is to functionalize it with ferrocene or methylene blue at the 3′ and by immobilization of alkane thiol, alkane amino, streptavidin, and hydrazoate molecules at 5′ ends of the DNA strand. By observing the electrochemical change on the electrode surface, it is possible to determine the change in DNA aptamer construction. To detect interferon-gamma (IFN-gam), Liu et al. created a biosensor based on a 34-mer IFN-binding aptamer in electrochemical mode. The linear detection range of the sensor was amplified up to 10 nM, and the LOD was 0.06 nM [31]. Similarly, Chen et al. used conventional semiconductor techniques to create a biosensor array based on the same aptamer used in previous study modified with MB and disulfide. This electrochemical sensor had LOD of 1.3 ng/mL, this sensor was able to pick up IFN- in the 1 to 500 ng/mL linear range [32].

1.4.4 Biomimetic Biosensor:

To detect analytes (such as glucose, proteins, or DNA) in a sample, biomimetic biosensors are sensors that mimic the structural integrity and functional behavior of biomolecules, such as enzymes and antibodies. They are frequently employed in environmental monitoring and medical diagnostics. They are created by using synthetic enzymes or biological molecules as recognition elements, coupled to transducers that transform the recognition event into an electrical signal. High specificity and sensitivity biomimetic biosensors are well known for their versatility in a variety of applications. A biological recognition element and an analyte are specifically bound by a biomimetic biosensor's operating principle. An electrode, optical fiber, or other type of sensing platform may be used as the transducer surface, which is where the biological recognition element, such as an enzyme or antibody, is immobilized. The recognition element binds to the analyte when it is present in the sample, changing the transducer signal. An electrical signal that can be amplified, filtered, and analyzed is then created from this change [33-35].

An enzyme-based biosensor, for instance, uses the enzyme to transform the analyte into a product that could be recognized by transducer. In an antibody-based biosensor, the antibody binds to a particular antigen, and a transducer can notice this interaction. Biomimetic biosensors can detect exceedingly tiny amounts of analytes with high sensitivity and specificity by using recognition elements. Bio-molecular

recognition events can also serve as the foundation for the operation of biomimetic biosensors. The transduction mechanism used by the biosensors can be direct or indirect. A measurable signal is produced by a bio-molecular recognition event in a direct transduction mechanism, whereas a measurable signal is ultimately produced by a cascade of reactions following a bio-molecular recognition event in an indirect transduction mechanism [35].

1.4.5 Potentiostatic Biosensor

Potentiostatic sensors are a particular classification of biosensors that measure the electrochemical activity of a biological recognition element using a process known as potentiostatic control. A method for preserving a constant electrode potential throughout a measurement is potentiostatic control. As opposed to this, a method known as galvanostatic control entails maintaining a constant current. The bio-recognition component i.e., an enzyme or antibody, is immobilized on an electrode surface in a potentiostatic biosensor. A steady potential is then given to the electrode while it is submerged in a solution containing the analyte. The subsequent quantification of the electrode's current as a function of time follows. A change in the rate of an electrochemical reaction causes a change in the current flowing through the electrode when the analyte binds to the recognition element. Electrochemical measurements like amperometry, voltammetry, and impedance spectroscopy frequently employ potentiostatic biosensors. Because of the high sensitivity and selectivity of these biosensors, they are effective for the detection of a wide range of analytes in several different industries, including biomedicine, environmental monitoring, and food safety [36, 37].

1.4.6 Amperometric Biosensor

A particular kind of biosensors that measures the current produced by an enzymatic or redox reaction using electrochemical amperometry are classified in this category of biological actuators. This method is based on measurement of electric current produced when an analyte is reduced or oxidized at a working electrode [38]. A biological recognition component, like an enzyme or an antibody, is immobilized onto the external interface of a functioning electrode in an amperometric biosensor. A continual potential is then applied to the working electrode while it is submerged in a solution containing the analyte. The subsequent measurement of the electrode's current as a function of time follows. A change in the rate of an electrochemical

reaction causes a change in the current flowing through the electrode when the analyte binds to the recognition element. Amperometric biosensors are frequently used to identify a wide range of molecules, including cholesterol, glucose, lactate, and other biomolecules. They are frequently employed in environmental monitoring, food safety, and medical diagnostics. Their benefits include low cost, high specificity, and sensitivity. Their drawbacks include the requirement for frequent calibration and interference from other chemicals in the sample, among others [39].

1.4.7 Conductometric Biosensor

Biosensors known as conductometric biosensors use conductometry, an electrochemical method, to gauge a solution's electrical conductivity. Based on the electrochemical reaction between the target molecule and the biorecognition element, this method measures the change in a solution's electrical conductivity. The biological recognition component, such as an enzyme or antibody, is immobilized on the surface of an electrode in a conductometric biosensor [40]. The electric conduction of the analyte-containing solution is then measured with the electrode submerged in the solution. The rate of an electrochemical reaction is altered when the target molecule binds to the recognition element, changing the conductivity of the solution. Conductometric biosensors are capable of detecting a wide range of analytes, including glucose, ions, and biomolecules, and are renowned for their high sensitivity and specificity. They are frequently employed in environmental monitoring, food safety, and medical diagnostics. Although conductometric biosensors are straightforward and inexpensive devices but their sensitivity and selectivity can be compromised by the presence of other ionic molecules in the solution [41, 42].

1.4.8 Optical Biosensor

When a recognition element interacts through an analyte, photosensitive biosensors use optical techniques to measure fluctuations in the physical or biochemical properties of the sample. These sensors are based on the idea that when a recognition element and an analyte interact, the sample's optical characteristics—such as its absorption, fluorescence, or phosphorescence change [43]. Optical biosensors can detect a variety of analytes, including proteins, DNA, and small molecules, and are renowned for their high sensitivity and specificity. They are frequently employed in environmental monitoring, food safety, and medical diagnostics. Although they are

quick and non-intrusive, they are also complex and susceptible to interference from other compounds in the sample [44, 45].

Optical biosensors come in a variety of forms, including:

- Fluorescence biosensors: These sensors use a molecule's or nanoparticle's fluorescence as a signal. When a molecule or nanoparticle binds to an analyte, the fluorescence intensity changes [46].
- SPR biosensors: These sensors depend on the change in SPR intensity brought on by an analyte's binding to a recognition element [47].

1.5 Introduction to the Components of Present Study

1.5.1 Interdigitated Electrodes for Biosensors (Platform)

Interdigitated electrodes (IDEs) are a type of electrode that entails of a sequence of thin corresponding fingers interdigitated with each other. These electrodes are commonly used in electrochemical biosensors, such as amperometric and potentiometric biosensors, to increase the active external area of the electrode and to advance the sensitivity and selectivity of the device [48]. The fingers of the IDEs are typically made of a conductive material, such as gold or platinum, and are detached by a slight slit. The active area of the electrode is increased by the large figure of fingers, which increases active sites for the recognition element, such as enzymes or antibodies, to bind to the analyte [49]. The IDEs can be fabricated using several techniques, such as photolithography, electrodeposition, and laser ablation, which allows for accurate control over the geometry and size of the fingers. IDEs are commonly used in biosensors for glucose, lactate, and other biomolecules detection. They are also used in sensing devices for electroanalysis, electrocatalysis, and in the field of energy storage such as supercapacitors. The small gaps between the fingers also allow for better mass transport of the target molecule to the active sites, which improves the sensitivity of the sensor [50, 51].

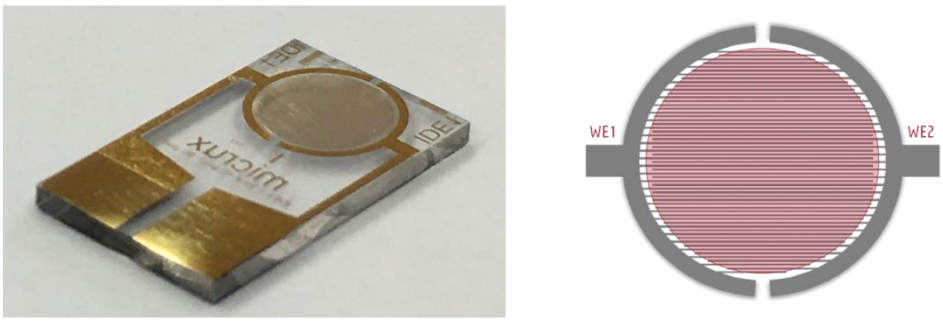

Figure 3: Typical structure of a Gold IDE (a) with enlarged working area (b).

IgG is a significant class of antibodies that is capable of being detected using interdigitated electrodes (IDEs). IgG plays a significant part in the immune system's reaction to infections and disorders. The electrodes are first modified with a recognition element, such as an anti-IgG antibody, that selectively binds to the IgG in

the sample to detect IgG using IDEs. This can be accomplished via several methods, including covalent bonding, adsorption, and self-assembling monolayers.

The electrodes are then submerged in a solution containing the IgG sample after the recognition element has been immobilized on the IDEs. The IDEs can detect a change in the electrical signal because of the IgG in the sample adhering to the electrodes' identification element. It is possible to quantitatively calculate the amount of IgG present using this shift in signal, which is proportional to the concentration of IgG in the sample.

There are diverse ways of measuring the electrical signal depending on the type of biosensor. For example, in amperometric biosensors, the change in current flow through the electrode is measured, while in potentiometric biosensors, the change in potential difference between the electrode and a reference electrode is measured. IDEs can be used in both types of biosensors and allow to detect IgG at low concentrations and with high specificity. This type of biosensors has potential applications in medical diagnostics, such as the detection of certain diseases and infections, and in the biotechnology industry for the detection of antibodies in therapeutic protein production.

1.5.2 Perfluoro decanethiol (Anchoring Element)

Perfluorodecane thiol (PFDT) is a liquid crystal compound that consists of a perfluorodecane hydrocarbon tail and a thiol head group. It is often used as a model compound to study the self-assembly and phase behavior of surfactants and lipids. Due to its hydrophobic tail and hydrophilic head, it can form various phases such as micelles, vesicles, and liquid crystals, depending on the conditions such as temperature, concentration, and pH [52, 53].

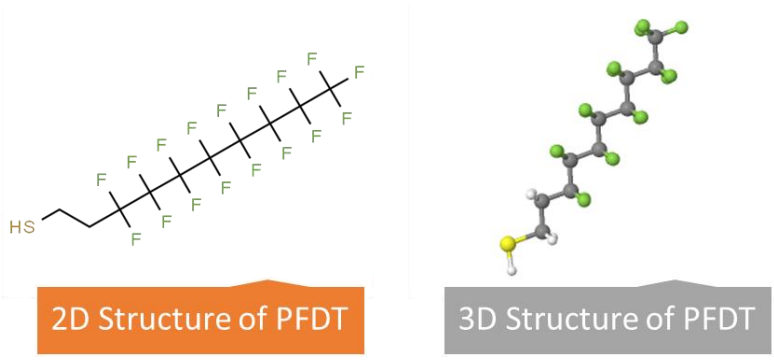

Figure 4: 2D and 3D structure of a PFDT molecule.

PFDT has been extensively used in several applications such as in the fabrication of biosensors, drug delivery systems, and in the optical and electronic fields. Its liquid crystal phases can be used as a model for the formation of functional materials such as gold and silver nanoparticles, and for the immobilization of enzymes, proteins, and DNA. SAMs of PFDT can be used in several applications such as in biosensors, bioelectronics, and in the field of surface chemistry. They can be used as a template for the formation of functional materials such as gold and silver nanoparticles, and for the immobilization of enzymes, proteins, and DNA. Additionally, the liquid crystal properties of PFDT can also be utilized in liquid crystal displays and in the field of self-assembling monolayers.

[54, 55].

Additionally, the liquid crystalline properties of PFDT makes it an ideal material for use in liquid crystal displays, which are widely used in electronic devices such as smartphones, televisions, and computers. The thiol group in PFDT also makes it useful in the field of surface chemistry and self-assembling monolayers, as it can be used to form stable and well-defined monolayers on various surfaces. The liquid crystalline properties of PFDT can also be modified by chemically modifying the thiol head group or by blending it with other compounds, which expands its potential applications [56].

A self-assembled monolayer (SAM) of perfluorodecane thiol (PFDT) is a thin film of the compound that is formed spontaneously on a surface when it is exposed to a solution of the compound. The process is driven by the chemical interactions between the thiol head group of the PFDT molecules and the surface, which results in the formation of a dense, ordered, and stable monolayer on the surface.

When a solution of PFDT is dropped on a surface such as gold, silver, or other metals, the thiol groups of the PFDT molecules react with the surface atoms, forming covalent bonds between the thiols and the surface atoms. This results in the formation of a monolayer of PFDT on the surface. The ordered and stable monolayer can be characterized by various techniques such as ellipsometry, XPS, and AFM. The chemical properties of the thiol head group of PFDT can be modified by chemical modification, which expands the potential applications of the SAMs. SAMs

of PFDT can be prepared in a controlled manner, providing a uniform and well-defined surface, which makes it an attractive material for various applications [57].

1.5.3 Aptamer 8 (Biorecognition Element)

An aptamer is a single-stranded nucleic acid, such as DNA or RNA, which has a high affinity and specificity for binding to a given target molecule. Since they replicate the binding characteristics of antibodies, they are frequently referred to as "artificial antibodies." A technique known as "systematic evolution of ligands by exponential enrichment" can be used to choose aptamers from a collection of random sequences. (SELEX). A protein, a tiny molecule, or a cell are examples of specific targets that aptamers are frequently used for. [58].

Aptamers have been used in a wide range of applications such as biosensors, drug delivery, and therapeutics. They have several benefits over traditional antibodies such as smaller size, chemical stability, and the ability to be synthesized in copious quantities. They also have the ability to cross cell membranes which allows them to target intracellular proteins and other biomolecules [59].

Aptamer 8 refers to a specific aptamer that has been isolated from a library of random sequences using SELEX. The target of Aptamer 8 is not specified in the information provided, so it is unclear what it specifically binds to. Aptamers are often named based on the order in which they were isolated during the selection process, and the specific name of Aptamer 8 refers to its place in the order of aptamers discovered.

1.5.4 IgG (Analyte)

Immunoglobulin G (IgG) is a type of antibody that plays a key role in the immune response to infections and diseases. It is the most abundant type of antibody in the blood and is found in all body fluids. IgG is a gamma globulin protein that is made up of four polypeptide chains, two heavy chains and two light chains. IgG is the only antibody that can cross the placenta and provide passive immunity to the fetus. It also provides long-term immunity to a specific antigen and is responsible for the secondary immune response. IgG is also the most important antibody for preventing infections caused by bacteria and toxins [60].

IgG antibodies can be used in medical diagnostics, such as the detection of certain diseases and infections. They can also be used in the biotechnology industry for the detection of antibodies in therapeutic protein production. The measurement of IgG levels in blood can also be used as an indicator of the overall health of an individual's immune system. The detection of IgG can be performed using various techniques such as ELISA, Western Blot, Immuno-fluorescence, Immuno-radiometry, and other techniques. ELISA is the most common method used for detection of IgG and other antibodies. ELISA can be used to detect IgG in different body fluids such as serum, plasma, or saliva .

1.5.5 Importance of IgG

Immunoglobulin G (IgG) is an important class of antibodies that plays a key role in the immune response to infections and diseases. IgG is the most abundant type of antibody in the blood and is found in all body fluids. It is the only antibody that can cross the placenta and provide passive immunity to the fetus, and it is also responsible for providing long-term immunity to a specific antigen [61].

IgG antibodies are important in the body's defense against bacterial infections, as they can neutralize toxins and help to remove bacteria from the body. They can also activate the complement system, which is a cascade of proteins that work together to help destroy bacteria and other foreign invaders. IgG is also important in the diagnosis of certain diseases and infections. The measurement of IgG levels in blood can be used as an indicator of the overall health of an individual's immune system. IgG can also be used to detect specific pathogens or antibodies, such as in the diagnosis of HIV, Hepatitis B and C, Lyme disease, and other infections [62].

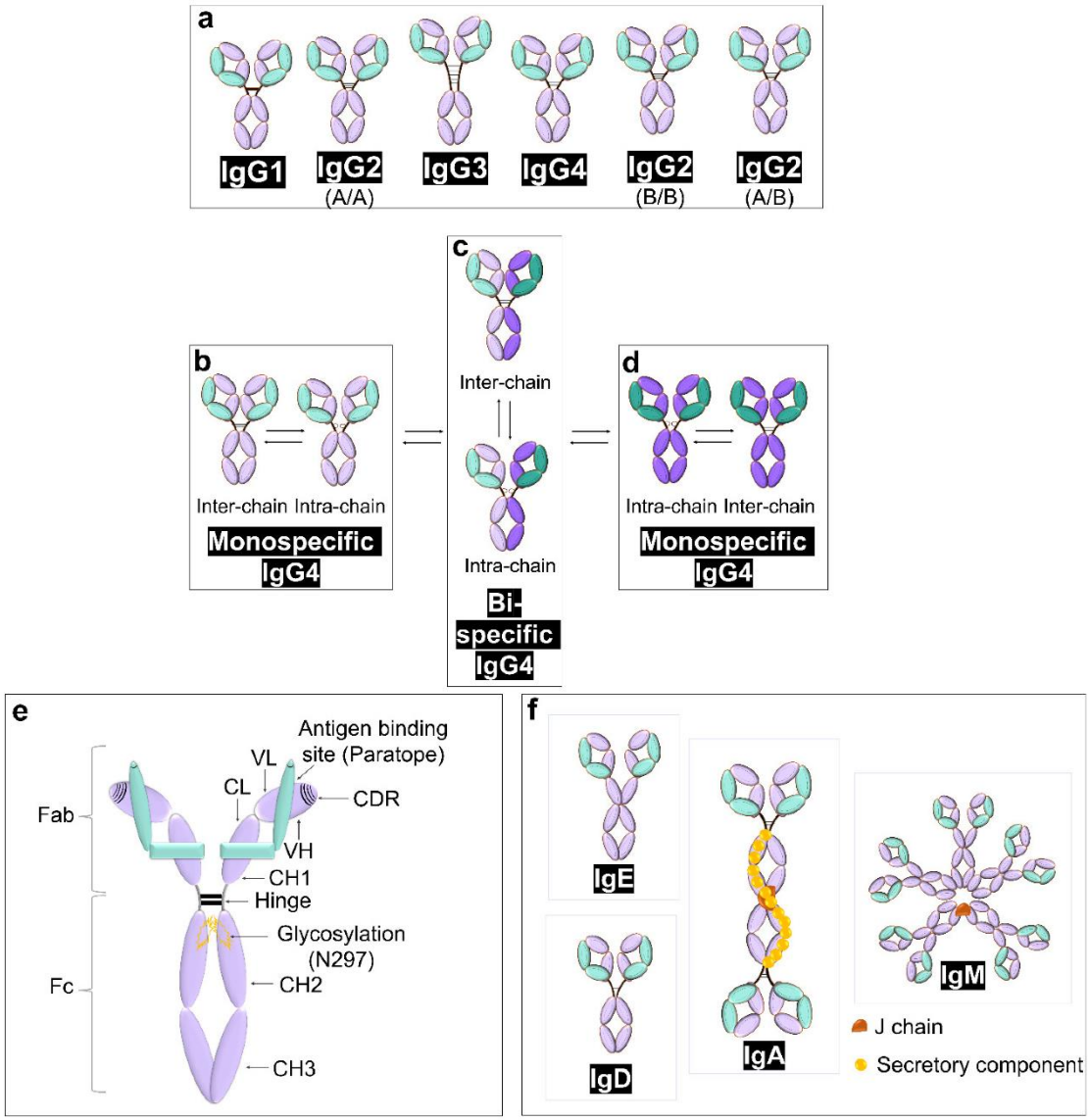

Figure 5: This figure illustrates the structural differences between the four IgG subtypes and allotypes (a-d). These variations arise from differences in the hinge region as well as in the heavy and light chains. The antigen specificity of IgG is determined by the complementarity determining regions (CDRs) shown as striped lines. The glycosylation patterns depicted in yellow have an impact on IgG function. The light chain (green) and heavy chain (purple) are also shown. Additionally, the figure provides a comparison of IgG structures with other immunoglobulins (f). Adapted from [61, 63-65].

1.6 Objectives

- To analyze the effects of various experimental circumstances on sensor performance and to improve the sensor preparation utilizing SAMs of PFDT.
- To determine if modified Aptamer-8 may be used as a sensing component for the effective detection of IgG antibodies.
- To evaluate the modified Aptamer-8 sensor's sensitivity and limit of detection for detecting IgG antibodies in various samples.
- To examine potential uses of the PFDT and aptamer-8 sensor in clinical diagnostics for the detection of IgG antibodies and propose future strategies for advancements in the said sensing platform.
- To compare the performance of the modified Aptamer-8 sensor with existing methods for IgG antibody detection through literature review.

Chapter: 2

Literature Review

2.1 Biosensing of IgG

Biosensing of IgG refers to the detection and measurement of immunoglobulin G (IgG) antibodies using biosensors. IgG is the furthermost abundant category of antibody in the bloodstream and plays an integral part in the immune system's response to pathogens. Biosensors for IgG can be used in multiple applications, including disease diagnosis, research, and food safety testing. Different biosensing techniques, such as optical, electrochemical, and piezoelectric, can be used to detect IgG. These techniques work by binding the antibodies to a sensor surface and then measuring a physical or chemical change that occurs because of the binding.

2.1 Electrochemical Biosensing of IgG

These types of sensors measure the analytical signals generated by an electrochemical signal. A good amount of research has been conducted to advance a robust and simple sensor to detect IgG and a part of that research will be summarized in this portion. Axin Liang A. et al. have successfully constructed a sensitive and discerning sensor using MIP (Molecularly Imprinted Polymer) for the IgG biorecognition. The role of a composite containing disulfide of molybdenum and quantum dots along with nitrogen doped graphene and ionic liquids has been studied for the signal amplification of sensors in this same study. This unique sensor was as rapid as its response time was less than 8 minutes and as sensitive as its LOD was 0.02 ng·mL−1 (Liang, Hou et al. 2021). In another research, Liang A. et al. used copper MOF (Metal-organic framework) with a LOD of up to 3 pg mL-1 [66]. Zarei H. et. al. developed a stable sensor based on magnetic nanocomposite composed of COOH-modified multiwalled CNTs (COOHMWCNTs) plus goat anti-human IgG (anti-hIgG) for the detection of human tetanus IgG antibody. This sensor was stable for up to one month with a LOD of 25 ng/ml [67]. Chen M. et. al. designed a strategy for biosensor antifouling with the help of Y-shaped peptides which were able to recognize IgG with the lowest concentration detection up to 32 pg/ml [68]. During the recent outbreak of corona virus, the standing of the SARS-CoV-2 IgG detection was emphasized for this disease diagnosis and prognosis. Liu H. et. al.

used an OECT (organic electrochemical transistors) based platform for viral antibody (SARS-CoV-2 IgG) detection which was able to respond in several minutes with the detection range of 10 fM to 100 nM [69]. A selective method for IgG detection with detection bound of 2.8 pg/ml was reported by Yuan L. et. al. which was based on a ferrocene-labeled immunoassay [70]. Barman SC. et. al. used PAAMI (polyelectrolyte polyallylamine) for the first time along with laser ablated graphene (LAG) and produced a sensitive actuator for point of care recognition of IgG where the salient feature of this sensor was its LOD up to 6 pg/ml [71]. This is not all, Medhi A. at. al. has deposited a composite made up of graphene oxide, conductive polymer, and Au-NPs onto ITO electrode for IgG recognition. This specific model had a inclusive detection range from 9 to 363 ng/ml and a limit of 49 ng/ml [72]. Also, bovine serum albumin (BSA) linked polymer nanowires has also been exploited to be used for electrochemical sensing of IgG having a detection limitation down to 0.27 ng/ml. Polyaniline polymer was used for the reduction of biofouling in this specified biosensor and this platform can further be explored [73]. Bai R. et. al. reported a simple and non-toxic biosensor of IgG detection by using IgG imprinted polymers decorating on the surface of gold electrode which was further decorated with nano gold and nano nickel and least concentration to be measured by this electrode was 2.0 mg/ml [74]. Another reported biosensor has a particularly good LOD and sensitivity of 0.18×10−19%V/V and 2.14 $\mu A.\%V/V.cm^{-2}$, respectively. Because of such a good sensitivity, the said biosensor was able to differentiate SARS-CoV-2 antibodies in plasma from other interfering antibodies [75].

In a different study, scientists developed a human (H)-IgG immunosensor using a low-cost and incredibly simple manufacturing approach based on nanorods of Zinc Oxide (ZnO-NRs) which were produced by the electrodeposition method. The ZnO-NRs had a reduced graphene oxide (rGO) layer electrodeposited on them to aid antibodies anchoring. The immunosensor's assessment of the hydrogen development reaction's current density and the H-IgG concentration were indirectly connected. By building the calibration curve in this way, a detection range of 10-1000 ng/mL with a low LOD and high sensitivity was obtained [76].

2.2 Uses of Perfluoro decanethiol in Biosensors

A plasmonic substrate made up of 3D nano-popcorn was made using surface energy amid an Au layer and PFDT spacer. Due to the energy differential, the self-assembly of Au nanoparticles formed numerous hotspots on the substrate due to the nearby nanoparticles. Due to the homogenous dispersal of numerous hotspots at the nano-popcorn platform, localized plasmonic effects significantly boosted the incidence field at hotspots, enabling repeatable target molecule characterization. This SERS-based aptasensor was calculated to have a LOD of 97 PFU mL-1 and an assay duration of 20 min for the detection of A/H1N1 virus [54]. Yet in another study self-assembled pillar arrays of NPs were used to detect influenza virus-related antibodies. The 3D plasmonic chip has structural integrity which makes it superior to unstructured gold substrates hence it has 100 times higher detection sensitivity towards influenza antibodies. The growth of plasmon-enhanced sensing applications is made possible by the simple and mountable manufacture of extremely responsive 3D plasmonic nanostructures [77]. An innovative biosensor assay based on the concept of immobilizing ACE2 in an amphiphobic layer is based on findings from another work and is sensitive, selective, and scalable. This sensor test offers selectivity for two proteins (interleukin-6 and streptavidin) and sensitivity to recombinant spike protein (1.68 ng mL1). The platform was examined by using the inactivated corona virus and a LOD of 38.6 copies mL-1 was observed. Investigating using a clinical sample with a high viral load (Ct = 26) after inactivation in VPSS medium showed robust discrimination against a negative sample. By using glucose biosensor invention methods which are economical, it is possible to provide a clear path to translation using proven manufacturing techniques, use of current sensor substrates, and usage of readout devices with prior CE registration. Together, our results point to an important diagnostic method that may be used to swiftly and cheaply check for SARS-CoV-2 in a range of contexts [78]. Two-dimensional (hydrophilic) channels were created on films made of cellulose nanofibrils using photolithography and inkjet printing. hIgG was used as a target analyte in this study and it was tested after surface alteration with either bovine serum albumin (BSA), globulin, or block copolymers of PDMAEMA (poly2-dimethylamine ethyl methacrylate) and POEGMA (polyoligoethylene glycol methyl ether methacrylate) [79]. The design, assembly, electrochemical behavior, rust behavior, and tribological features of fluor organic monolayers absorbed on copper were examined in a

different study. Using a self-assembling technique, thin films of PFDT were grafted onto copper. The monolayer of fluor organic SAMs' fluorine groups gives the ultrathin film remarkable lubricating characteristics. Additionally, SAM grafting enhanced the surface wear resistance. One of the most exciting lubricants for copper appears to be PFDT SAMs because they enhanced the mechanical characteristics of surface by lowering its friction and erosion [56, 80]. PFDT is reported to have antibiofouling properties as well [78, 81].

2.3 Uses of Aptamer 8 in Biosensors

The SELEX method commonly known as Systematic Evolution of Ligands by Exponential Enrichment, was independently developed in vitro by three groups in 1990 and is used to select aptamers for various targets [82-84]. Selection, separation, and amplification are the three primary methods that can be used to choose aptamers from a random library of nucleotides either ssDNA or RNA (usually 1015–1016 separate sequences). Depending on the structural features of aptamers, they can be employed in various applications i.e., target identification [85-87]. The elevated affinity and tunable properties of aptamers allow them to be a potential candidate in the field of analyte diagnostics, and the transducer has a considerable effect on their sensitivity. The progression of aptamer-based biosensors has been the subject of countless publications published up to this point. The synthesis of aptamer based biosensors used a number of methods, including optical (optical aptasensors based on fluorescence and colorimetry), electrochemical biosensors, chemiluminescent, and surface-enhanced Raman scattering (SERS) aptasensors [88-91]. Electrical and optical aptasensors are the two categories of aptasensors that employ aptamers. In biosensors, aptamers are frequently employed to identify pathogens like viruses and bacteria. The following figure illustrates how an aptamer-based biosensor works in general. Optical aptasensors make use of optical principles for detection. The aptamers perform numerous optical functions as signal-transduction elements or as other sorts of biorecognition components [92]. The advantages of this family of aptasensors include low cost, terrific sensitivity, robustness, and easy labelling [93]. A few techniques with photosensitive aptasensors include fluorescence, chemiluminescence, SPR, SERS, and colorimetric techniques [94]. Electrical aptasensors produce electrical signals when analyte and bioreceptor interact. These aptasensors feature an easy, quick detection method, great sensitivity, and low

detection limits [95]. When analyte and bioreceptor interact, electrical aptasensors generate electrical signals. These aptasensors are simple to use, have a speedy detection process, and have low detection limits [96].

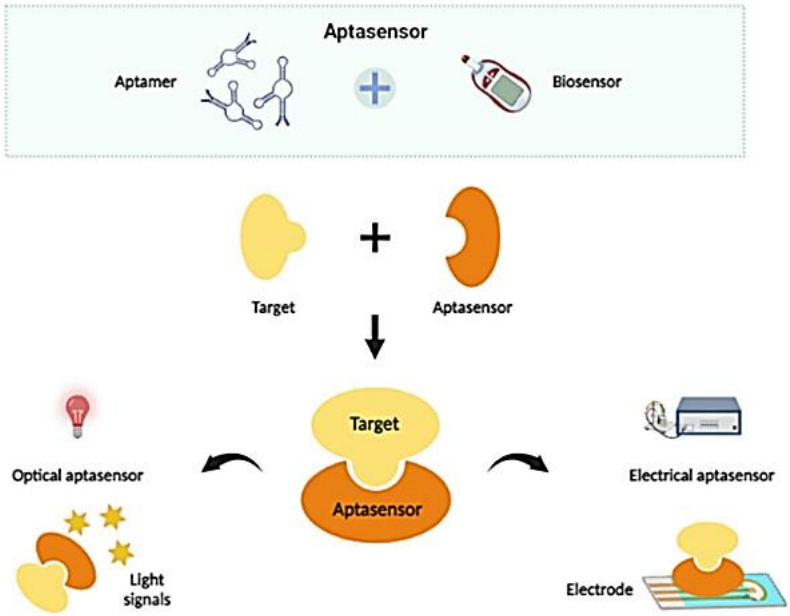

Figure 6: General working principle of an aptamer biosensor.

Aptamers have many positive attributes that make them promise for therapeutic use. However, there are also several limitations that restrict their effectiveness in vivo. One of these drawbacks is their susceptibility to nuclease degradation, which can result in in vivo half-lives of less than 10 minutes. To address this issue, modifications have been made to the nucleic acid structure of aptamers. Certain regions, such as the ends of nucleic acid chains, nucleoside sugar rings, and phosphodiester links, have been modified to resist nuclease degradation. These modifications aim to increase the stability and duration of aptamer activity in vivo, improving their therapeutic potential [97]. One of the limitations of aptamers in vivo is their small size, which makes them vulnerable to elimination by renal filtration. To overcome this issue, larger molecules, such as proteins or cholesterol, can be attached to the 5'-end of aptamers to increase their size. For example, Lee et al. modified a 29-nucleotide-long, 20-F pyrimidine-modified RNA aptamer by conjugating it with cholesterol, resulting in a cholesterol-conjugated aptamer. This modification increased the aptamer's resistance to nuclease degradation and extended its half-life [98, 99]. Despite some of the limitations of aptamers, the advancement of aptamer-selection technology has been made possible by the application of

enhancement techniques. Although the diagnostic and therapeutic industries currently benefit greatly from this technology, further research is required to create additional aptamers for practical use. Aptamers can be used in commercial kits to provide quick, simple, and affordable detection, and they can be applied not only in biomedical disciplines but also in agriculture and aquaculture to identify infections that can cause food poisoning. Furthermore, the selection process of aptamers must be improved to enable the simultaneous identification of multiple targets, rather than just one. The stability and sensitivity issues of aptamers need to be addressed in the future to improve their analytical performance [100].

While the diagnostic and therapeutic industries currently benefit greatly from this technology, further research is required to create additional aptamers for practical use. Aptamers have the potential to be utilized in commercial kits to provide rapid, affordable, and simple detection, not only in biomedical disciplines but also in agriculture and aquaculture to identify infections that can cause food poisoning. Additionally, the selection process of aptamers needs to be improved to enable the simultaneous identification of multiple targets. The stability and sensitivity issues of aptamers must be addressed in the future for improved analytical performance. In another study, an optical biosensor for the detection of corona virus spike proteins was developed which consisted of three main components including S-protein complimentary aptamer, a photoactive material and Au NPs/Yb-TCPP. The high sensitivity and low detection limit of 72 ng/ml was reported [101]. The combination of aptamer with nanomaterials is able to give more robust devices as in a study the nanocrystalline diamond (as working electrode) were used for the label free biosensing of IgE. The aptamer was modified with the amino terminal while diamond nanostructures was functionalized with -COOH functional group and these chemical modifications helped in the covalent attachment of both components. EIS was conducted to study the electrochemical behavior of this biosensor and results suggested that the double layer capacitance of electrode was proportional to the concentration from 0.03 g/mL to 42.8 g/mL and LOD was found to be 0.03 g/mL

The NCD-based aptasensors demonstrated exceptional selectivity, even in the presence of a significant IgG excess, and produced consistent signals during six renewal cycles. The successful testing of the impedimetric aptasensor on serum samples suggests the potential for using EIS for the label-free, direct measurement of

IgE levels in human serum samples [102]. FRET biosensors have also evolved due to the usage of aptamers as a thrombin detection sensor was proposed by T. Patois et al. They have used an aptamer which was labelled with dye made up of graphene. Because aptamer and graphene lack covalent adhesion, the dye's fluorescence is quenched due to FRET. During the addition of thrombin, the recovery of fluorescence was observed by the formation of a unique complex known as quadruplex-thrombin. This biosensor had unique quenching ability which made it highly sensitive and selective towards in vitro samples and in vivo sample studies. The graphene aptasensor had higher sensitivity than CNTs aptasensor as it has quiet lower limit of detection approximately about 31.3 pM [103]. A new homogeneous electrochemical aptamer-based biosensor was developed for thrombin detection using electrically aided bonding and tetra ferrocene signal amplification. Unlike other sensors, this aptasensor does not require any electrode modification and employs a simple probe for efficient detection. Tetra ferrocene, a signal marker consisting of four ferrocene molecules, was used to mark the probe's terminal position, which provides a higher amplification indication for the recognition of thrombin. The aptamer probe, which has a stem-loop structure, was labelled with tetra ferrocene and thiol at the 3′ and 5' terminals, respectively, to detect thrombin. The thiol group could not reach the electrode surface when it was enclosed within the stem-loop structure, even with applied voltage. However, upon exposure to the thrombin target protein, the stem-loop structure unfolded, allowing the rapid adsorption of the thiol group to the electrode surface, leading to potential-assisted self-assembly of Au-S. The tetra ferrocene electrochemical signal was measured using DPV and demonstrated a low detection limit of 0.126 pM with high specificity for single mismatch detection [104]. Another novel electrochemical biosensing platform has been developed for the simultaneous detection of various targets using split aptamers and exonuclease I cleavage. The flexible and label-free platform detected targets with precision by forming a ternary complex that was resistant to degradation by exonuclease I, resulting in a significant output of impedance. The aptasensor was able to successfully detect thrombin, adenosine triphosphate, and mercury ion with sensitivity and selectivity, with detection limits of 32 fM, 1.43 pM, and 1.65 pM, respectively. This approach offers a simple and efficient tool for detecting multiple targets, demonstrating potential for use in disease diagnostics and environmental monitoring [105].

2.4 IDEs Based Biosensors

The unique sensing properties of IDEs have made them a potential candidate for the biosensing industry, and they have grabbed the attention of thousands of scientists and they are convinced to carry out research on these sophisticated electrodes. For instance, an affinity based DNA detection biosensor was proposed in a study and this capacitive sensor had the capability to detect up to 20 molecules of complementary DNA and a lower concentration of 1.5 aM range. This has helped us to make this proposal a suitable one for point of care detection process of other molecules too. Apart from that this biosensor consisted of 24-nucleotide DNA probes which was based on a virus known as West Nile and this specific viral strain is known as Kunjin strain. The other highlighting point of this platform was its high reproducibility and it was enhanced by the immobilization of ssDNA oligomers onto gold interdigitated surface [106].

In a study, a sensing system based on reduced graphene and (rGO) field-effect transistors (FETs) customized with a particular aptamer was used to detect the HPV-16 E7 protein. The authors reported good covalent coupling of the aptamer using EDC/NHS and emphasized the significance of the attachment technique for the ligand. With a detection limit of 100 pg mL-1 (1.75 nM) and a dissociation constant (Kd) of 200 nM, real-time monitoring of aptamer-protein interaction revealed preferential binding of HPV-16 E7. In this study, aptamers are used as particular recognition elements to show the potential of rGO-based FETs for the sensitive detection of proteins [107].

Comparable results were obtained in another work that used composites of PEDOT-Poly(allylamine hydrochloride) (PAH) as the channel material for the successful production of Organic Electrochemical Transistors (OECTs). The ability to tune both the electrical and ionic characteristics while retaining high transconductance values, a key factor in the creation of high-performance bioelectronic devices, was made possible by controlling the ratio of polyelectrolyte to PEDOT. Lower threshold voltages and the ability to run the transistors at low gate voltages—both of which are necessary for successful integration with biological systems—were produced by the introduction of PAH into the channel material. The highest pH sensitivity was achieved by adding pH-sensitive amino moieties to the PEDOT-PAH1 OECTs, and an enzyme named AchE was effectively functionally electrostatically anchored. The

resulting biosensors could track acetylcholine in the 5-125 m range. The inclusion of several enzymes on the channel material, according to the authors, could result in the creation of devices that can monitor distinct biomarkers in real-time. The development of tools capable of concomitant neurotransmitter detection and electronic recording of brain signals may result from the integration of PEDOT-PAH OECTs in neuromorphic circuits and their capacity to recognize acetylcholine [108].

Chapter: 3

Materials and Methodology

2.5 Chemicals

The chemicals used in this study include Gold IDEs from Micrux Technologies, Sulphuric acid (98%) from RCI Labscan, Ethanol (washing grade), Hydrogen peroxide (35%) from MERCK, Potassium Hexaferocyanide from Sigma Aldrich, KCl (EMSURE), Phosphate Buffer Saline from Life Technologies, Perfluorodecane thiol from MACK, Toluene from Riedel-de Haën, Aptamer 8 from Integrated DNA technologies, and IgG. These chemicals were used for various experimental procedures and were purchased from reputable companies to ensure high quality and reproducibility of results. Careful attention was given to proper storage and handling of each chemical in accordance with the manufacturer's recommendations.

2.6 Characterization Equipment

Several characterization techniques were employed in this study to investigate the physical and chemical properties of the samples. The contact angle was measured using the Drop shape analyzer-DSA25 from KRUSS to determine the wetting behavior of the samples. ATR-FTIR (Agilent Cary 630 FTIR Spectrometer) was used to study the chemical composition of the samples and to analyze the functional groups present. The surface morphology of the samples was studied using SEM (JOEL JSM-6490LA) and AFM (JSPM-5200), which provided high-resolution images of the surface topography. XRD (Seimens D5005 STOE & Cie GmbH Darmstadt, Germany) was used to identify the crystalline phases present in the samples. Additionally, the electrochemical behavior of the samples was investigated using a Gammry Potentiostat (Gamry Interface ® 1010E) to measure their electrochemical properties. Each characterization technique was carefully selected based on the information needed to address the research questions and was performed using appropriate parameters and settings to ensure accurate and reproducible results.

2.7 Methodology

2.7.1 Washing of IDEs

Before being functionalized, IDEs were cleaned and activated in accordance with the company's protocol (MICRUX Technologies), which included dipping in piranha solution (H_2SO_4:H_2O_2 in a 3:1 ratio) and then producing hydrogen and oxygen electrochemically to clean the metal surface of dust particles. The IDEs were chemically cleaned by being sonicated for 30 minutes in each of the solvents: Piranha solution, DI water, absolute ethanol, and Electrochemical cleaning was carried out after drying in a drying oven by running CV between -1.0 and +1.3V at a sweep rate of 100mV/s with 0.05M H_2SO_4 as the background electrolyte. Each IDE took 10 minutes to complete the 12 cycles of electrochemical washing and completely cleaned IDEs were dried in the drying oven for further use.

2.7.2 PFDT Solution and SAM Preparation

To successfully get PFDT SAM onto IDEs working area, first PFDT was added into toluene under constant magnetic stirring until a 1 mM solution was formed. The floruos effect in the PFDT helps in phase separation. Afterwards, IDEs were put in PFDT solution to cover their working area in the Eppendorf tubes for 24 hours. The next day each IDE were washed with DI water for 10 seconds with the help of wash bottle to rinse off unbound molecules and left to dry in glove box with Nitrogen environment [109].

2.7.3 Anchoring of Aptamer 8

Each IDE received a 200 mL aliquot of Aptamer 8 that had been diluted from stock in 1 x PBS to a range of concentrations before being incubated for an hour at room temperature. The IDEs were then dried with nitrogen flow after being rinsed with 1 x PBS for 10 seconds per electrode.

2.7.4 Incubation with IgG

To investigate the possibility of specific binding between Aptamer 8 and IgG, a series of IgG dilutions were incubated at room temperature for one hour on the sensor area of the IDEs. After incubation, the electrodes were rinsed with 1 x PBS using a water bottle flow for 10 seconds per electrode to remove any unbound

molecules. This step was crucial in determining the evidence of specific binding between the aptamer and IgG.

2.7.5 Electrochemical Studies parameters

All electrochemical studies including were carried out using KCl (0.1 M) salt within PBS (1X), and $[Fe(CN)6]^{3-/4-}$ as redox couple (5mM) [110] and three electrode system was used throughout the series of experiments i.e. Ag/AgCl (reference electrode), Pt wire (counter electrode) and IDE (working electrode) as done in previous studies [111, 112]. All the electrochemical studies were conducted at maximum current of 0.5 mA.

Table I: Parameter for electrochemical testing

Technique	Parameters
CV	Potential Window (-1 V to 1 V) Scan Rate (100 mV/s) Step Size (2 mV)
EIS	DC Voltage (0 V) AC Voltage (10 mV) Frequency Range (100 KHz-0.01 Hz)
DPV	Initial E (-0.4), Final E (0.8), Sample Period (5s)
SWV	Initial E (-0.4), Final E (0.8), Sample Period (5s)

Chapter: 4

Results and Discussion

3.1 Contact Angle

The wetting behavior of the IDEs surface was studied using contact angle measurement. Prior to the surface modification, the IDEs showed a contact angle of 83 degrees, indicating moderate hydrophobicity. After the deposition of PFDT-SAM, the contact angle increased significantly to 120 degrees (Figure 2a and 2b), suggesting a highly hydrophobic surface. This increase in contact angle can be attributed to the hydrophobic nature of PFDT and its uniform distribution on the IDEs surface [113].

Subsequently, Aptamer 8 was used to functionalize the PFDT-modified IDEs surface, and the contact angle was measured again. As shown in Figure 2c, the contact angle decreased significantly, indicating an increase in surface hydrophilicity. This result can be attributed to the hydrophilic nature of Aptamer 8, which has a high affinity for IgG [114]. Furthermore, several dilutions of IgG were incubated on the biosensor, and the contact angle was measured again. As expected, the contact angle decreased further (Figure 2d), indicating an even more hydrophilic surface due to the presence of IgG. These results suggest that the biosensor surface is highly responsive to the presence of IgG and can be used for sensitive and selective detection of this biomolecule.

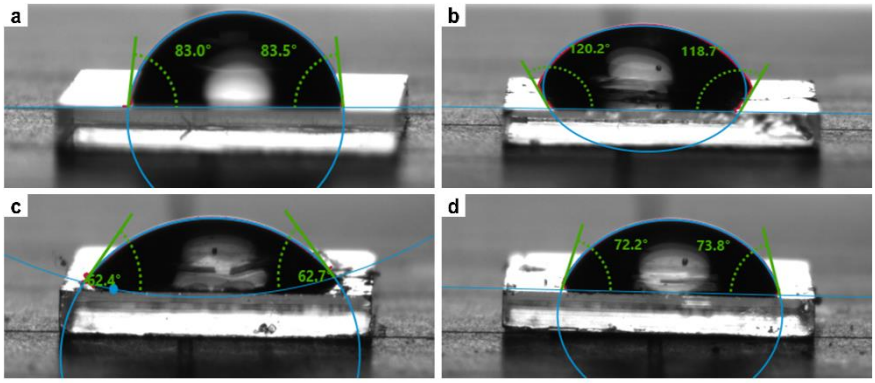

Figure 7: Concat angle measurements of Bare-IDE (a), PFDT-IDE (b), Apt.8-PFDT-IDE (c) and IgG-Apt.8-PFDT-IDE (d). The contact angle of b is greater of all the samples due to the hydrophobic nature of PFDT while aptamer 8 and IgG incubation reduced this angle down to 62.4 degrees and 72.2 degrees respectively.

3.2 XRD

The bare and functionalized electrodes were examined to look for the elemental analysis and crystal structures. The peak of bare IDE was matched with JCPDS card in Xpert high score, and it was a hundred percent match with gold (111) with 2 theta value at 38 degrees. The peak intensity of the other three samples PFDT-IDE, Apt.8-PFDT-IDE, and IgG-Apt.8-PFDT-IDE was seen to be reduced which can occur due to a phenomenon known as surface-induced structural changes. The PFDT monolayer can affect the intensity of the gold peak by altering the electron density around the gold atoms in the interdigitated electrode, which leads to changes in the intensity of the diffraction peaks. In particular, the PFDT monolayer can cause a decrease in the intensity of the gold peak due to its insulating properties and the fact that it covers some of the gold atoms in the electrode.

When the biomolecules adsorb onto the gold surface, they can undergo conformational changes that can affect their XRD pattern. Additionally, the presence of the biomolecules on the surface can also create a more disordered surface structure, which can also contribute to a reduction in peak intensity in the XRD pattern. In general, biomolecules such as aptamers, antibodies, and proteins do not typically give additional peaks in X-ray diffraction (XRD) analysis when absorbed onto a substrate such as a gold surface. Instead, the presence of the biomolecules on the surface can affect the intensity and/or shape of existing peaks, as well as create a more disordered surface structure, which can contribute to a reduction in peak intensity. However, in some cases, specifically when the biomolecules are crystallized, it is possible for them to show extra peaks in XRD analysis, but it is not a common scenario as biomolecules are mostly in amorphous form.

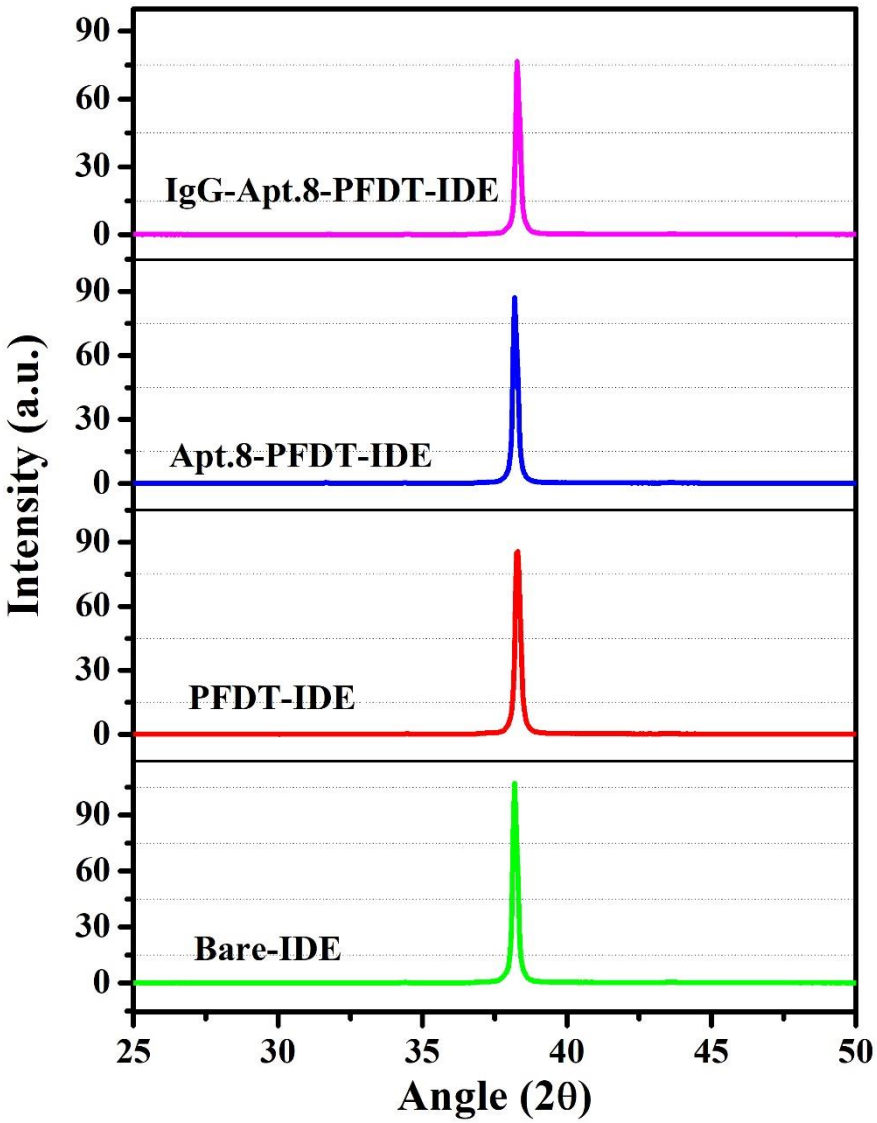

Figure 8: XRD peaks of Bare-IDE, PFDT-IDE, Apt.8-PFDT-IDE, and IgG-Apt.8-PFDT-IDE where difference is seen in the intensities of Au (111) peak for all samples. This peak is more intense in Bare-IDE because of changes in the intensity of the diffraction peaks.

3.3 SEM

The SEM analysis is a powerful imaging technique that allows for the visualization of surface features and morphologies. In this study, SEM analysis was used to investigate the surface morphology of the bare gold interdigitated electrode (IDE) and the modified IDEs, including PFDT-IDE, Apt.8-PFDT-IDE, and IgG-Apt.8-PFDT-IDE. The SEM analysis revealed that the bare IDE had some ridges on its surface, which could be attributed to multiple washing steps during the preparation of the electrode. On the other hand, the PFDT-IDE surface was uniform, smooth, and continuous with a thin and homogeneous film of PFDT molecules covering the entire surface of the gold electrodes. This confirms that the PFDT molecules are self-assembling and form a well-ordered monolayer on the IDE surface, without any visible defects or gaps in the coverage [77].

In the case of Apt.8-PFDT-IDE and IgG-Apt.8-PFDT-IDE, uniform ridges were observed on the surface of the PFDT monolayer. This indicates that the aptamer molecules were successfully immobilized onto the PFDT monolayer, resulting in a modified surface with a unique morphology. However, individual aptamer or IgG molecules were not visible under the imaging conditions used in this study. It is important to note that the details of the aptamer's conformation and the individual nucleotides or base pairs in the aptamer may be visible under different imaging conditions. The SEM analysis provides valuable information about the surface morphology of the modified IDEs and confirms the successful surface modifications with PFDT, aptamer 8, and IgG.

In summary, the SEM analysis confirmed the successful modification of the gold interdigitated electrode surface with PFDT, aptamer 8, and IgG. The PFDT monolayer was found to be uniform, continuous, and free of defects or gaps, which indicates the effectiveness of the self-assembly process. The uniform ridges observed on the surface of Apt.8-PFDT-IDE and IgG-Apt.8-PFDT-IDE suggest that the aptamer molecules were successfully immobilized onto the PFDT monolayer, resulting in a modified surface with a unique morphology. SEM analysis is a powerful technique for visualizing surface features and morphologies and provides valuable information about the effectiveness of surface modification strategies.

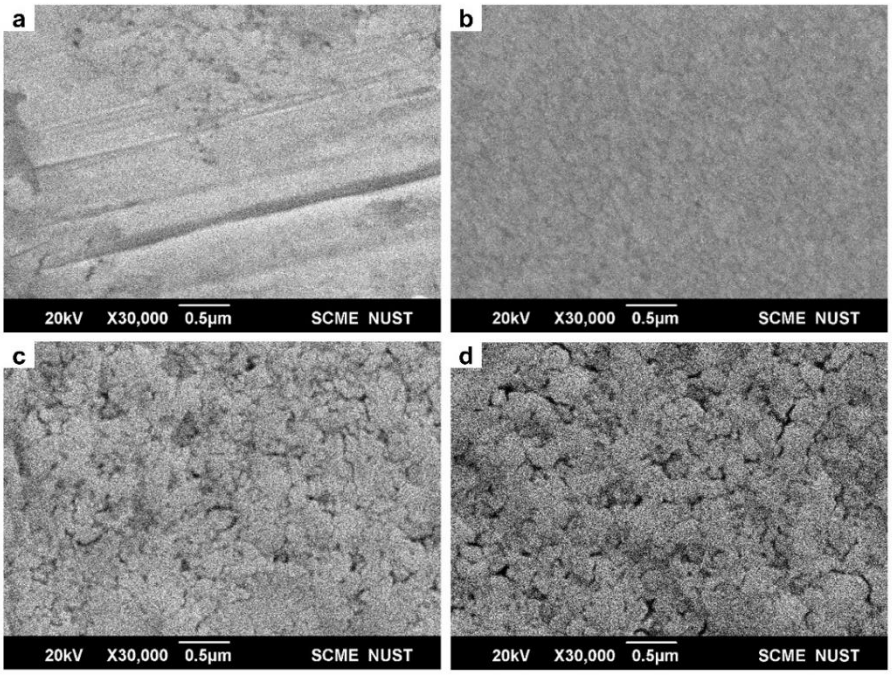

Figure 9: SEM images of Bare-IDE (a), PFDT-IDE (b), Apt.8-PFDT-IDE (c) and IgG-Apt.8-PFDT-IDE (d) on 30k resolution.

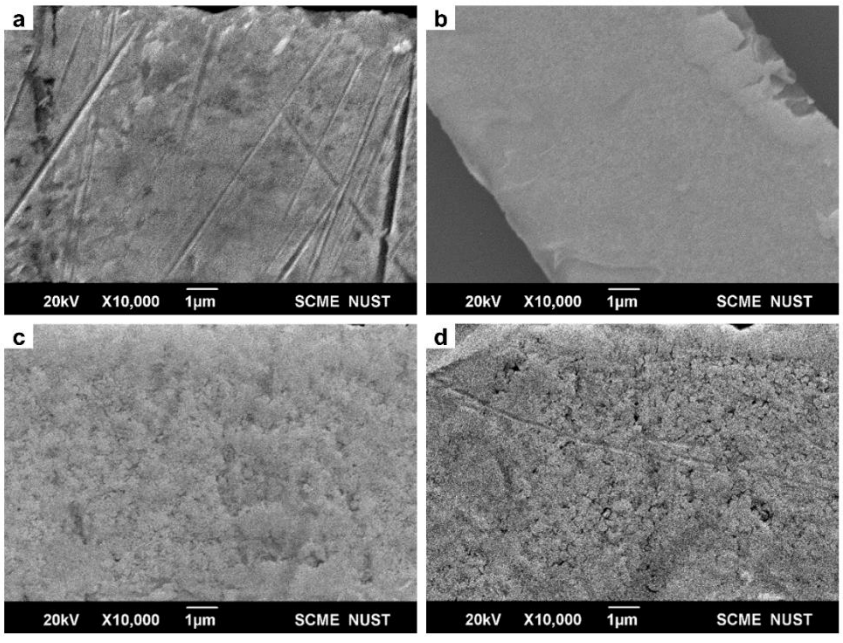

Figure 10: SEM images of Bare-IDE (a), PFDT-IDE (b), Apt.8-PFDT-IDE (c) and IgG-Apt.8-PFDT-IDE (d) at 10k resolution.

3.4 ATR-FTIR

The ATR-FTIR technique is a powerful tool for analyzing the functional groups present in a sample. In this case, the technique was used to analyze samples of a gold interdigitated electrode (IDE) both before and after modification. The resulting spectra showed several characteristic peaks, indicating the presence of various functional groups. One of the most prominent peaks observed in the spectra was the stretching vibration of the carbonyl group, which appeared at a frequency of 2158 cm-1. This peak is typical of molecules containing a carbonyl group, such as ketones, aldehydes, and carboxylic acids. Additionally, a peak at 2032 cm-1 indicated the presence of a C=O group, which is also commonly found in carboxylic acids and other organic compounds. Another important peak observed in the spectra was a C=C bond at 1977 cm-1. This peak is typical of molecules containing a carbon-carbon double bond, such as alkenes and aromatic compounds. A peak at 1100 cm-1 indicated the presence of a C-O bond, which is often found in alcohols, ethers, and esters.

In addition to these common functional groups, several peaks were also observed at specific frequencies that are characteristic of certain molecules. For example, a peak at 923 cm-1 indicated the presence of a C-H bond, which is typical of alkanes and other hydrocarbons. A peak at 1654 cm-1 indicated the presence of a -COOH bond, which is found in carboxylic acids. Finally, a peak at 1557 cm-1 indicated the presence of a nitrile bond, which is common in organic compounds such as amides and amino acids. Interestingly, all these peaks were observed in the spectra of all the samples analyzed, including the bare gold IDE as well as the modified PFDT-IDE, Apt.8-PFDT-IDE, and IgG-Apt.8-PFDT-IDE samples. The defined peaks of the PFDT, aptamer 8 and IgG functional groups were not observed because of the lower concentration of all these components used for each sample. There is typically a minimum concentration of a functional group that is required to be detectable by FTIR spectroscopy. The sensitivity of FTIR spectroscopy depends on the strength of the absorption of the functional group, which is related to the concentration of the functional group in the sample. In general, a higher concentration of the functional group in the sample will lead to a stronger absorption signal, which will be easier to detect. Contrary to that, the characteristic peak

of bare IDE at 1100 cm^{-1} was gradually seen to deintensify after each modification and peak at 1250 cm^{-1} was seen to be intensify after each modification. This suggests that these functional groups are either present in the starting material or are formed because of the modification process. Overall, the ATR-FTIR spectra provides.

valuable information about the chemical composition of these samples, which can be used to guide further analysis and characterization.

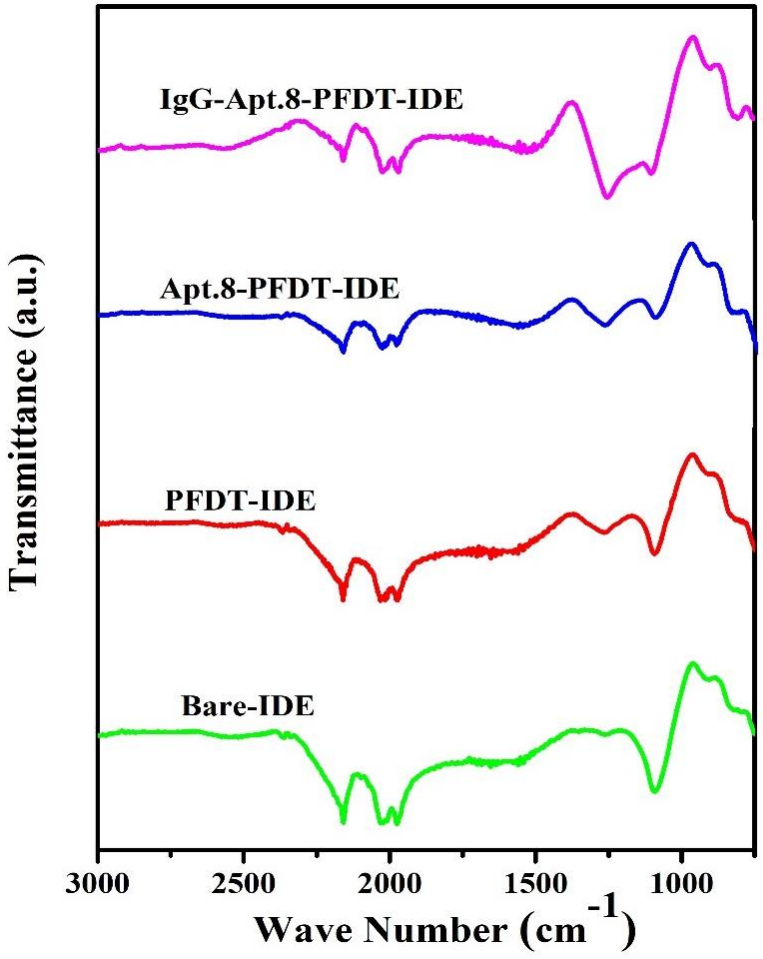

Figure 11: ATR-FTIR peaks of Bare-IDE, PFDT-IDE, Apt.8-PFDT-IDE, and IgG-Apt.8-PFDT-IDE.

3.5 AFM

The AFM technique is a powerful tool for analyzing the surface roughness and topography of solid surfaces, and it was used to analyze all samples including bare and modified electrodes. In this case, the AFM analysis was used to study the surface properties of the gold IDE before and after modification with PFDT, aptamer 8 and IgG. The AFM analysis revealed that the surface roughness of the bare IDE was higher compared to the modified IDEs. The surface coverage of PFDT molecules on the IDE surface was high, and the monolayer was found to be uniform. This resulted in a lower height profile in the 3D AFM image, indicating a smoother surface compared to the bare IDE. The reduction in surface roughness can be attributed to the ability of the PFDT molecules to form a self-assembled monolayer on the IDE surface, effectively filling in the gaps and crevices and creating a more uniform surface.

The height profile of an electrode is influenced by numerous factors such as the sample, the method of application, the thickness of the PFDT layer, the surface roughness, and other physical properties of the electrodes. In this case, the reduction in surface roughness can be attributed to the formation of a well-ordered monolayer of PFDT on the IDE surface. Aptamer 8, on the other hand, is a much longer molecule than PFDT, typically consisting of several hundred nucleotides in length. The length of the aptamer may vary depending on the specific sequence. The AFM analysis did not provide any specific data on the length of the aptamer, but it is expected to have a more significant impact on the height profile of the IDE compared to the smaller PFDT molecules.

Overall, the AFM analysis provides valuable information about the surface properties of the IDEs and how they are affected by modification with PFDT and aptamer 8. The reduction in surface roughness and the formation of a uniform monolayer of PFDT on the IDE surface demonstrate the effectiveness of this modification strategy in improving the surface properties of the IDE. The impact of aptamer 8 on the height profile of the IDE is expected to be more significant due to its larger size, which highlights the importance of considering the physical properties of the modifying molecules when designing surface modification strategies.

Table II: Rq values of Bare-IDE, PFDT-IDE, Apt.8-PFDT-IDE, and IgG-Apt.8-PFDT-IDE obtained by AFM analysis.

Samples	**Rq**
Bare-IDE	3.98
PFDT-IDE	0.853
Apt.8-PFDT-IDE	1.75
IgG-Apt.8-PFDT-IDE	7.45

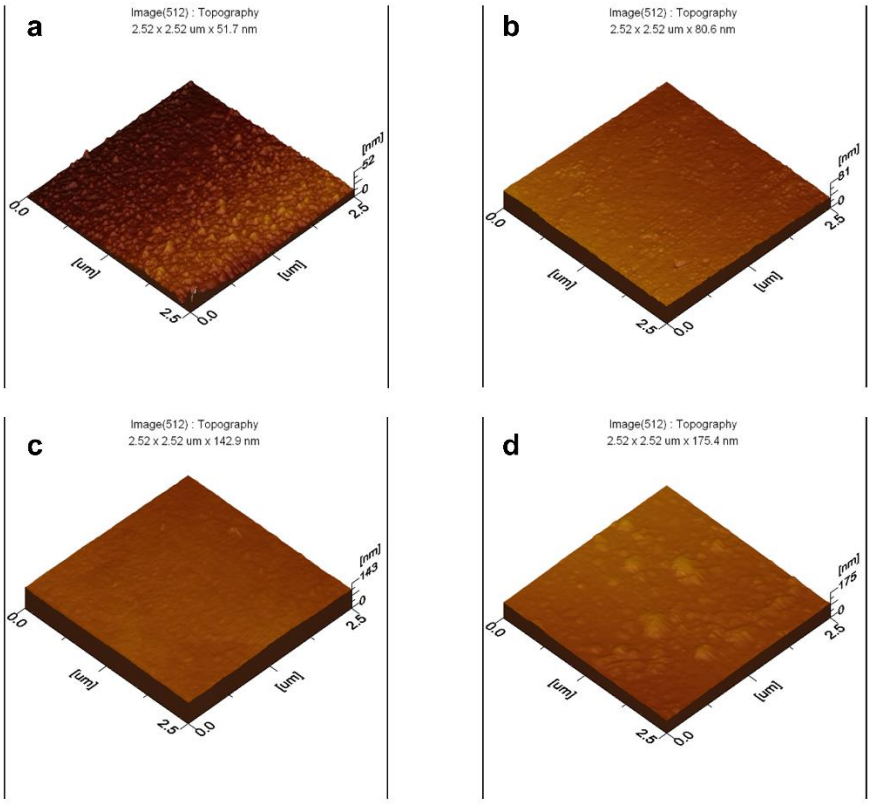

Figure 12: 3D images of Bare-IDE (a), PFDT-IDE (b), Apt.8-PFDT-IDE (c) and IgG-Apt.8-PFDT-IDE (d) obtained by AFM analysis.

3.6 Electrochemical characterization of samples

3.6.1 Confirming the deposition of PFDT

Two different concentrations of PFDT (1 mM and 2.5 mM) were used for the SAM deposition, and the resulting surfaces were characterized using electrochemical methods, including CV, EIS, and DPV. The results showed that increasing the concentration of PFDT led to an increase in the number of PFDT molecules being deposited onto the IDE surface. However, this also led to an increase in the resistance of the resulting SAM, as shown in Figure (b). This is because a thicker layer of PFDT increases the distance between the electrode surface and the electrolyte solution, leading to a higher resistance.

Furthermore, the total current flowing through the IDE decreased with increasing PFDT concentration, as shown in Figure (c). This is because the higher resistance of the thicker PFDT layer limits the flow of current through the IDE. Based on these findings, it was decided to use a lower concentration of PFDT (1 mM) for the SAM deposition. This concentration was previously reported in the literature and was found to provide enough PFDT coverage while still leaving some space for the aptamer 8 to bind to the IDE surface.

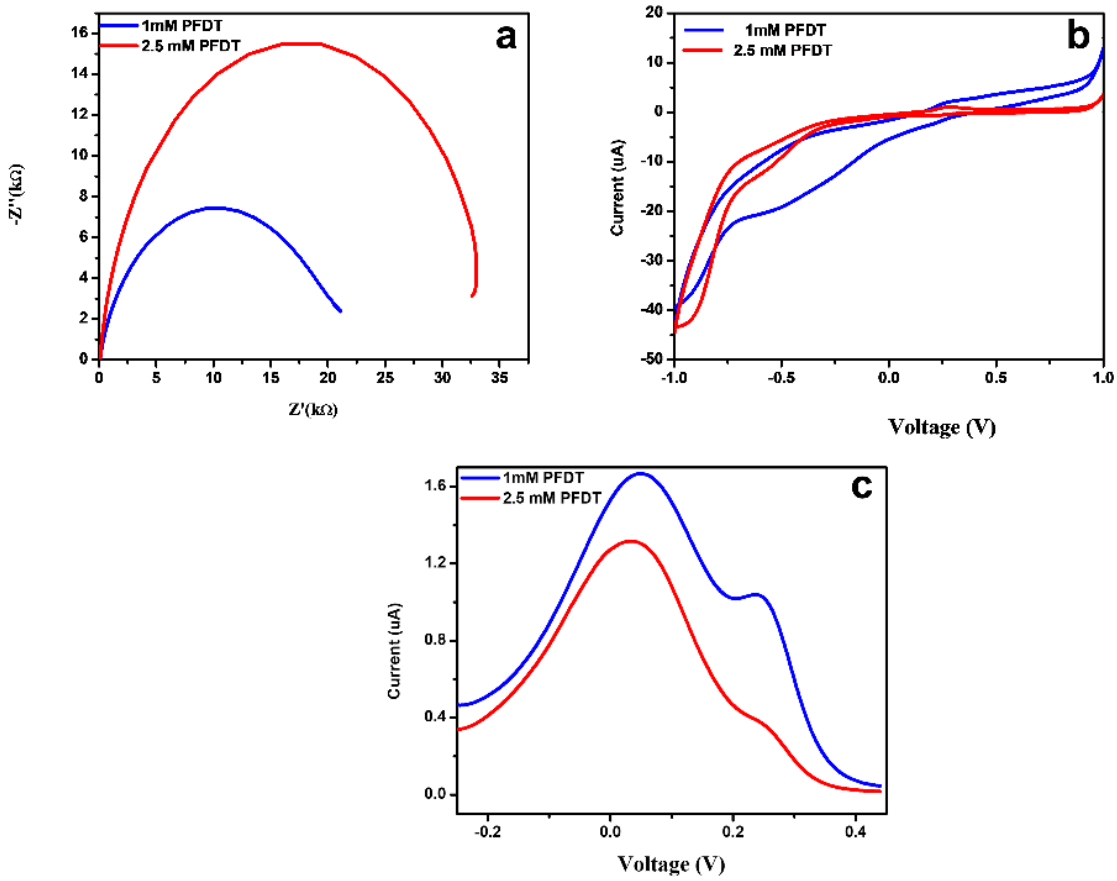

Figure 13: Electrochemical characterization of two different concentrations of PFDT (1mM: blue line, 2.5 mM: red line) via EIS (a), CV (b), and SWV (c). KCl (0.1 M) salt within PBS (1X), and [Fe(CN)6] 3-/4- as redox couple (5mM).

3.6.2 Effect of Layer-by-layer deposition of PFDT

In another way it was aimed to investigate the effects of depositing two layers of 1 mM PFDT on the electrochemical properties of interdigitated electrode arrays (IDEs). To achieve this, IDEs were immersed in a 1 mM PFDT solution for 24 hours, dried, and then immersed again in a fresh PFDT solution. Our results showed that after two incubations, the working area of the electrode was completely covered, which was evidenced by the presence of a loop in the cyclic voltammetry (CV) curve. Additionally, a high resistance and zero current were generated in the differential pulse voltammetry (DPV) curve, indicating successful deposition of PFDT on the IDEs surfaces.

These findings suggest that the deposition of PFDT on IDEs can have a significant impact on their electrochemical behavior. Specifically, the presence of PFDT may alter the surface chemistry of the IDEs, leading to changes in their electron transfer rate and affecting their electrochemical properties. The observation of a loop in the CV curve is consistent with the occurrence of redox reactions on the surface of the IDEs, which is due to the presence of the PFDT layer. Additionally, the high resistance and zero current observed in the DPV curve further confirm the successful deposition of PFDT on the IDEs surfaces.

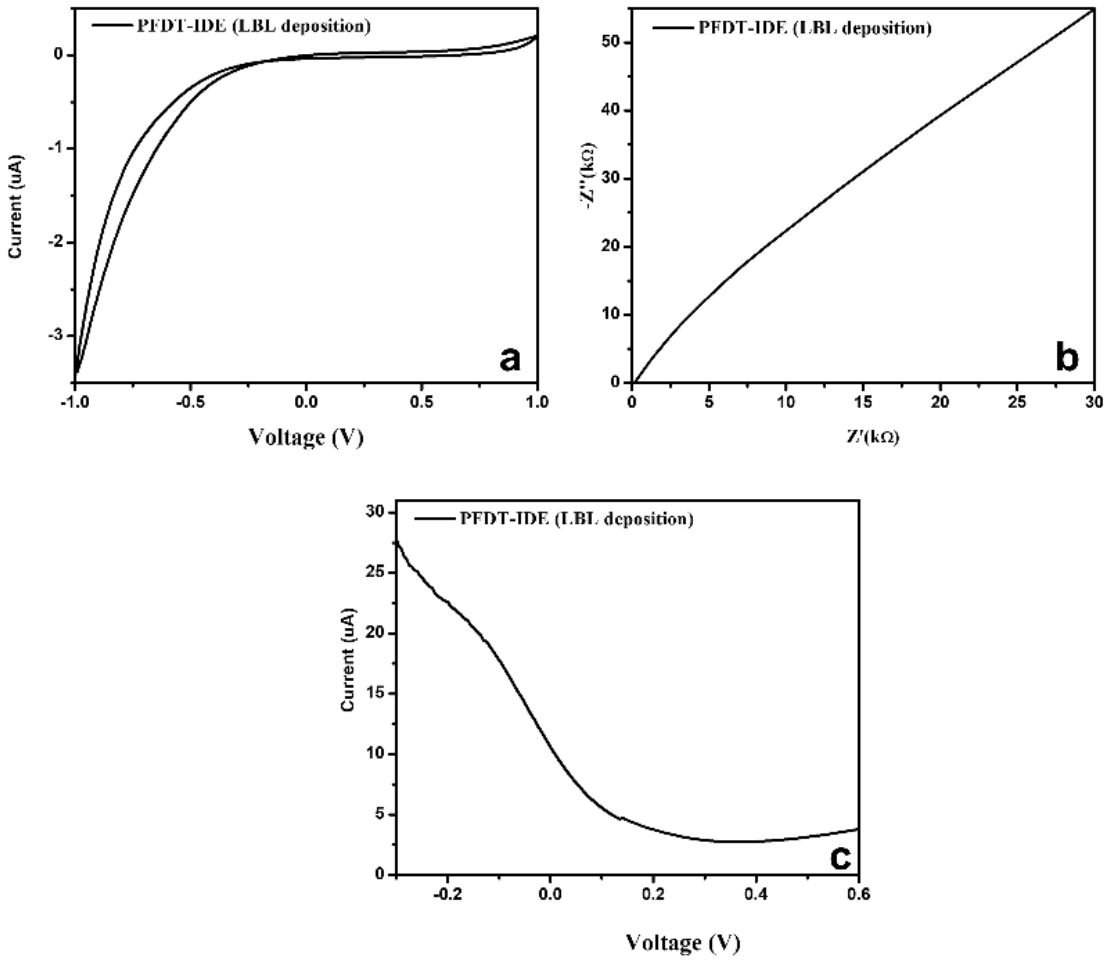

Figure 14: Electrochemical characterization of PFDT-IDE with two layers of PFDT-SAM via CV (a), EIS (b), and SWV (c). KCl (0.1 M) salt within PBS (1X), and [Fe(CN)6] 3-/4- as redox couple (5mM).

3.6.3 Aptamer Concentration Study:

After keeping the concentration of PFDT constant as 1 mM, different concentrations of the aptamer were incubated onto IDEs to investigate the effect of concentration on electrochemical properties of PFDT-IDE. It was revealed that increasing concentration of aptamer led to the decrease in current as can be seen in Figure 15 and 2ug/ml was the concentration that was used in further studies.

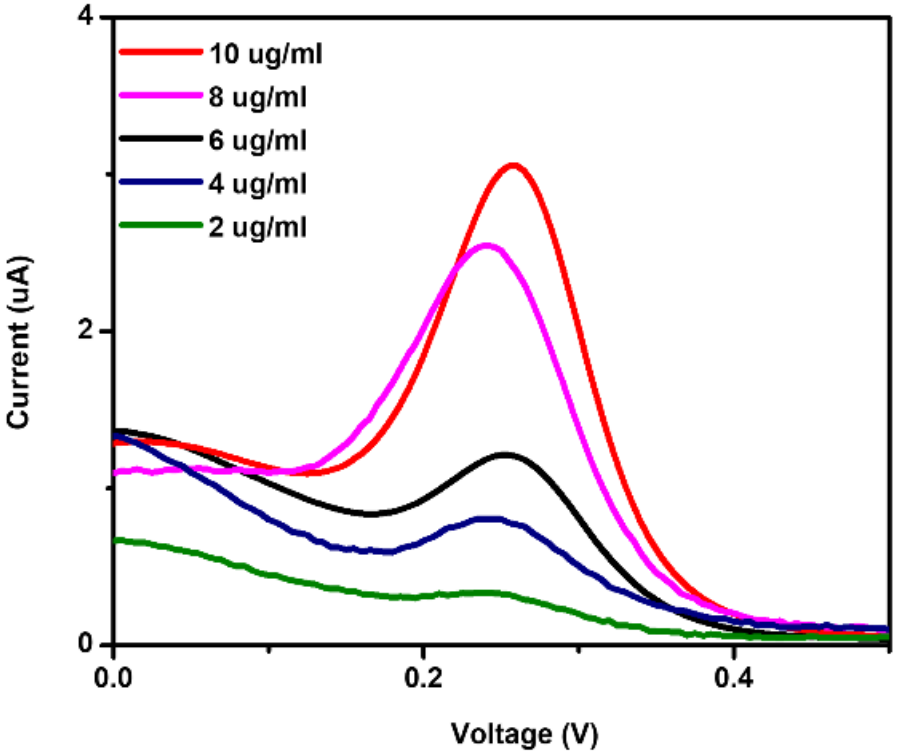

Figure 15: DPV results for various concentrations of aptamer 8. KCl (0.1 M) salt within PBS (1X), and [Fe(CN)6] 3-/4- as redox couple (5mM).

3.6.4 Aptamer Deposition and Electrochemical Studies

After the deposition of aptamer 8, a comparative study was conducted for bare, PFDT-IDE and Apt. 8-PFDT-IDE. The bare ide gave redox peaks while area under the cyclic voltammograms was reduced upon the deposition of PFDT as well as aptamer 8. The reason a cyclic voltammogram may not show oxidation and reduction peaks when PFDT is functionalized onto gold interdigitated electrodes (IDEs) is since PFDT forms a SAM on the surface of the gold electrodes, which can act as a barrier layer that prevents the oxidation and reduction of species in solution from occurring at the electrode surface. This is because the SAM is composed of highly ordered, densely packed molecules that can prevent the transport of electrons and ions to and from the electrode surface, effectively blocking the electrochemical reactions from taking place. Additionally, PFDT has a high electron-withdrawing ability and low electron-donating ability, this causes a low electron transfer rate and low electroactivity, which also leads to no or weak oxidation and reduction peaks observed in the cyclic voltammogram. Similarly, Aptamer sample deposition further covers the electrode area.

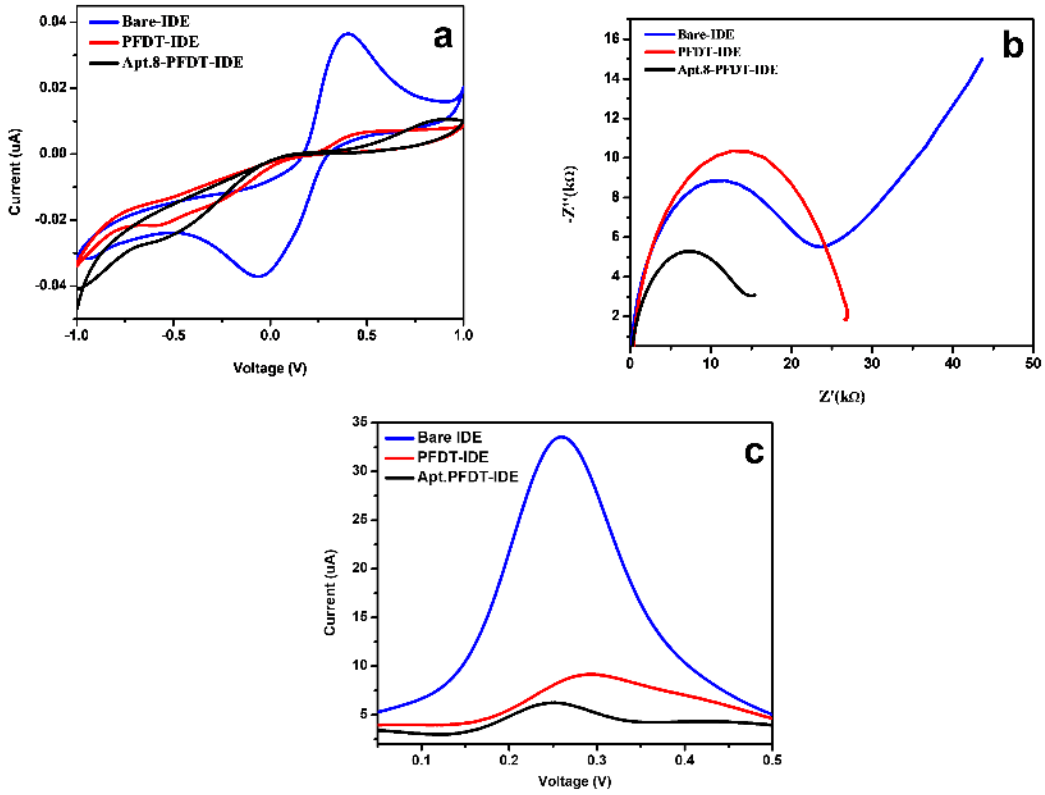

Figure 16: Electrochemical characterization of Bare-IDE, PFDT-IDE, and Apt.8-PFDT-IDE via CV (a,b), EIS(c), and SWV (d). KCl (0.1 M) salt within PBS (1X), and $[Fe(CN)_6]^{3-/4-}$ *as redox couple (5mM).*

3.7 Analyte recognition study

The response of a biosensing platform was evaluated by subjecting it to a range of dilutions of IgG, ranging from 0.25 µg/ml to 100 µg/ml. To measure the response, the electrical impedance spectroscopy (EIS) technique was employed for each IgG concentration. The results of this study revealed that the response of the biosensing platform was linearly proportional to the concentration of IgG. Specifically, as the concentration of IgG increased, the resistance of the biosensing platform also increased as depicted in figure 15.

This increase in resistance can be attributed to several factors. First, as the concentration of IgG increases, the amount of antigen-antibody binding sites also increases, resulting in a higher number of bound IgG molecules. This, in turn, causes an increase in the effective thickness of the sensing layer and an increase in the distance between the sensing electrode and the bulk solution. As a result, the diffusion of the electrolyte ions is hindered, leading to an increase in resistance.

Furthermore, at higher IgG concentrations, the binding sites on the sensing layer become saturated, resulting in a decrease in the number of available binding sites. This causes an increase in resistance as there are fewer available sites for further binding of IgG. Additionally, the formation of a densely packed IgG layer can lead to an increase in steric hindrance, further inhibiting the diffusion of electrolyte ions and increasing resistance.

In summary, the linear increase in resistance observed in the biosensing platform in response to increasing concentrations of IgG can be attributed to a combination of factors, including an increase in effective thickness, a decrease in available binding sites, and steric hindrance. These findings provide important insights into the behavior of biosensing platforms and their response to varying concentrations of analytes.

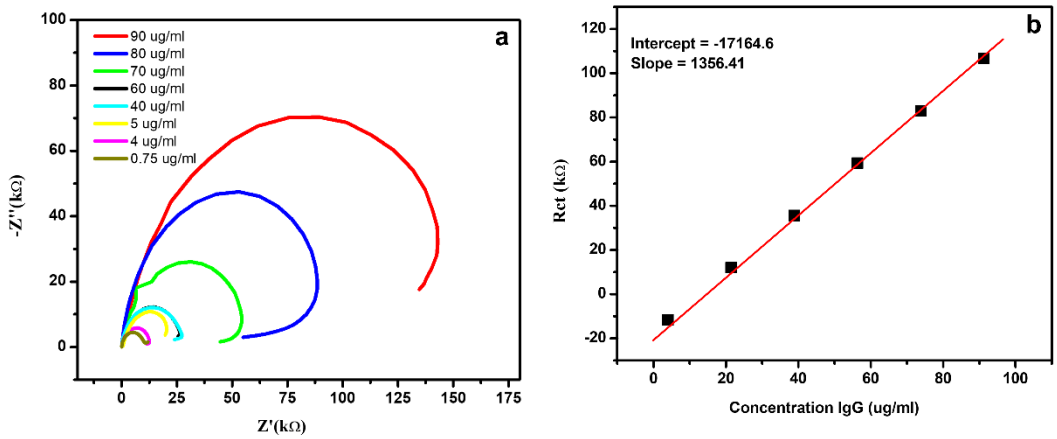

Figure 17: a represents the fitted data in Nyquist plots (EIS spectra) of faradaic measurements in KCl (0.1 M) salt within PBS (1X), and $[Fe(CN)_6]^{3-/4-}$ *as redox couple (5mM). The slope was 1356.41 which gave an estimated LOD of 13 ug/mL.*

3.8 Limit of Detection (LOD)

The lowest concentration of analyte that the measuring method can dependably detect is known as the LOD. The signal-to-noise ratio (S/N), which is the ratio of the peak current to the background noise, was calculated using EIS data to establish the LOD.

Using the following calculation, a detection limit (DL) of 13 ug/mL was determined in the current study.

$$\mathbf{DL= 3S.D/S}$$

where;

S.D is the standard deviation of the blank sample and S is the slope of the straight line.

The value of **S.D** from blank sample's Rct values (charge transfer resistance) values was calculated in excel and it happened to be **3135.156** while slope was calculated from calibration curve which was **1356.41**. Applying these values in the above equation;

$$\mathbf{DL= 3*3135.156 /1356.41}$$

$$\mathbf{DL=13.8\ ug/ml}$$

Conclusion

In the conclusion of the thesis, it can be stated that a two-step fabrication platform was successfully developed for the biosensing of IgG. This biosensing platform utilized PFDT and aptamer as anchoring elements and biorecognition elements, respectively. The use of these elements resulted in a sensitive and selective platform for the detection of IgG.

The modified gold IDE was characterized using various techniques to study the surface morphology and functional groups present on the surface. SEM and AFM were utilized to study the morphology of the modified IDE surface, while FTIR spectroscopy was employed to investigate the presence of functional groups on the surface.

Electrochemical studies were also conducted to investigate the response of the biosensing platform towards IgG. The platform exhibited a highly linear response towards varying concentrations of IgG, with a low limit of detection (LOD). The specificity of the biosensing platform towards IgG was also demonstrated using control experiments with non-specific analytes.

Overall, the developed biosensing platform demonstrated excellent performance characteristics, including high sensitivity, selectivity, and a low LOD of 13 ug/mL. The use of PFDT and aptamer as anchoring and biorecognition elements, respectively, proved to be a successful strategy for the development of an overly sensitive and selective biosensing platform for the detection of IgG. The characterization and electrochemical studies provided valuable insights into the behavior of the biosensing platform and its response towards IgG. These findings have important implications for the development of biosensing platforms for a variety of applications in clinical and diagnostic settings.

Future Aspects

The successful development of the two-step fabricated platform for the biosensing of IgG provides an excellent foundation for future research in this area. One potential avenue for future work could involve the optimization and fine-tuning of the biosensing platform to improve its sensitivity, selectivity, and reliability. This could be achieved using different anchoring and biorecognition elements, or through modifications to the surface chemistry of the platform.

Another potential area of future research could involve the development of biosensing platforms for the detection of other analytes of interest, such as other antibodies or biomolecules. The versatility and adaptability of the two-step fabrication platform make it well-suited for the development of biosensors for a wide range of applications.

Moreover, the biosensing platform developed in this project could be further integrated with advanced technologies such as microfluidics or nanoelectronics to improve its performance characteristics and expand its potential applications. The integration of these technologies could enhance the sensitivity and specificity of the platform, reduce the detection time, and enable the detection of multiple analytes in a single assay.

Finally, the biosensing platform developed in this project could be evaluated and validated using real-world samples to evaluate its performance in clinical and diagnostic settings. The platform's sensitivity and selectivity towards IgG could be further optimized for different biological matrices and fluids, such as blood, serum, or saliva, to enable the detection of IgG in different disease states.

Overall, the biosensing platform developed in this project holds enormous potential for future research and development in the field of biosensors and could have important applications in clinical and diagnostic settings.

References:

[1] Maitland, (2010) "A transdisciplinary definition of diagnosis," (in eng), *J Allied Health.* 39:306-13. vol. no. 4, p.^pp. Winter.

[2] Strimbu and Tavel, (2010) "What are biomarkers?," (in eng), *Curr Opin HIV AIDS.* 5:463-6. 10.1097/COH.0b013e32833ed177vol. no. 6, p.^pp. Nov.

[3] Perumal and Hashim, (2014) "Advances in biosensors: Principle, architecture and applications," *Journal of Applied Biomedicine.* 12:1-15. https://doi.org/10.1016/j.jab.2013.02.001vol. no. 1, p.^pp. 2014/01/01/.

[4] Abolhasan, Mehdizadeh, Rashidi, Aghebati-Maleki, Yousefi, and Bioelectronics, (2019) "Application of hairpin DNA-based biosensors with various signal amplification strategies in clinical diagnosis," 129:164-174. vol. p.^pp.

[5] Karimi-Maleh *et al.*, (2021) "A critical review on the use of potentiometric based biosensors for biomarkers detection," 184:113252. vol. p.^pp.

[6] Senf, Yeo, and Kim, (2020) "Recent advances in portable biosensors for biomarker detection in body fluids," 10:127. vol. no. 9, p.^pp.

[7] Nie, Yuan, Zhang, Chai, and Yuan, (2019) "Versatile and ultrasensitive electrochemiluminescence biosensor for biomarker detection based on nonenzymatic amplification and aptamer-triggered emitter release," 91:3452-3458. vol. no. 5, p.^pp.

[8] Banerjee, Maity, and Mastrangelo, (2021) "Nanostructures for biosensing, with a brief overview on cancer detection, IoT, and the role of machine learning in smart biosensors," 21:1253. vol. no. 4, p.^pp.

[9] Shabaninejad *et al.*, (2019) "Electrochemical-based biosensors for microRNA detection: Nanotechnology comes into view," 581:113349. vol. p.^pp.

[10] Shen, Wang, and Ke, (2021) "DNA Nanotechnology-Based Biosensors and Therapeutics," 10:2002205. vol. no. 15, p.^pp.

[11] Gu and Liu, (2020) "Introduction to biosensors," 8:3168-3170. vol. no. 16, p.^pp.

[12] Karunakaran, Bhargava, and Benjamin, *Biosensors and bioelectronics*. Elsevier, 2015.

[13] Thevenot, Toth, Durst, Wilson, and Chemistry, (1999) "Electrochemical biosensors: recommended definitions and classification," 71:2333-2348. vol. no. 12, p.^pp.

[14] Michelmore, "2 - Thin film growth on biomaterial surfaces," in *Thin Film Coatings for Biomaterials and Biomedical Applications*, H. J. Griesser, Ed.: Woodhead Publishing, 2016, pp. 29-47.

[15] Harvey, *Analytical Chemistry 2.0*. LibreTexts, 2010.

[16] Su, Jia, Hou, and Lei, (2011) "Microbial biosensors: A review," *Biosensors and Bioelectronics.* 26:1788-1799. https://doi.org/10.1016/j.bios.2010.09.005vol. no. 5, p.^pp. 2011/01/15/.

[17] Scheller and Schubert, *Biosensors*. Elsevier, 1991.

[18] Luong, Male, and Glennon, (2008) "Biosensor technology: technology push versus market pull," 26:492-500. vol. no. 5, p.^pp.

[19] Wang, (2008) "Electrochemical glucose biosensors," 108:814-825. vol. no. 2, p.^pp.

[20] Shavanova *et al.*, (2016) "Application of 2D non-graphene materials and 2D oxide nanostructures for biosensing technology," 16:223. vol. no. 2, p.^pp.

[21] Nikhil, Pawan, Nello, and Pedro, (2016) "Introduction to biosensors," 60:1-8. vol. no. 1, p.^pp.

[22] Perumal and Hashim, (2013) "ScienceDirect Advances in biosensors: Principle, architecture and," 12:1-15. vol. p.^pp.

[23] Newman and Setford, (2006) "Enzymatic biosensors," *Molecular Biotechnology.* 32:249-268. 10.1385/MB:32:3:249vol. no. 3, p.^pp. 2006/03/01.

[24] Lakard *et al.*, (2011) "Urea potentiometric enzymatic biosensor based on charged biopolymers and electrodeposited polyaniline," 26:4139-4145. vol. no. 10, p.^pp.

[25] Benhar, Eshkenazi, Neufeld, Opatowsky, Shaky, and Rishpon, (2001) "Recombinant single chain antibodies in bioelectrochemical sensors," 55:899-907. vol. no. 5, p.^pp.

[26] Wang *et al.*, (2022) "Development of the DNA-based biosensors for high performance in detection of molecular biomarkers: More rapid, sensitive, and universal," *Biosensors and Bioelectronics.* 197:113739. https://doi.org/10.1016/j.bios.2021.113739vol. p.^pp. 2022/02/01/.

[27] Keum and Bermudez, (2009) "Enhanced resistance of DNA nanostructures to enzymatic digestion," 7036-7038. vol. no. 45, p.^pp.

[28] Ma, Ali, Dodoo, and He, (2006) "Enhanced sensitivity for biosensors: multiple functions of DNA-wrapped single-walled carbon nanotubes in self-doped polyaniline nanocomposites," 110:16359-16365. vol. no. 33, p.^pp.

[29] Tan, Neoh, Kang, Choe, and Su, (2012) "Affinity analysis of DNA aptamer–peptide interactions using gold nanoparticles," 421:725-731. vol. no. 2, p.^pp.

[30] Bishop, Ren, Polander, Jeanfreau, Trent, and Chaires, (2007) "Energetic basis of molecular recognition in a DNA aptamer," 126:165-175. vol. no. 1-3, p.^pp.

[31] Liu, Tuleouva, Ramanculov, and Revzin, (2010) "Aptamer-based electrochemical biosensor for interferon gamma detection," 82:8131-8136. vol. no. 19, p.^pp.

[32] Chen, Pui, Kongsuphol, Tang, Arya, and Bioelectronics, (2014) "Aptamer-based array electrodes for quantitative interferon-γ detection," 53:257-262. vol. p.^pp.

[33] Nagel, Stone, and Watkins, (2009) "An overview of biomimetic sensor technology," *Sensor Review - SENS REV.* 29:112-119. 10.1108/02602280910936219vol. p.^pp. 03/27.

[34] Kozitsina, Svalova, Malysheva, Okhokhonin, Vidrevich, and Brainina, "Sensors Based on Bio and Biomimetic Receptors in Medical Diagnostic, Environment, and Food Analysis," *Biosensors*, vol. 8, no. 2. doi: 10.3390/bios8020035

[35] Rudnitskaya, "Sensors | Biomimetic Sensor Arrays," in *Encyclopedia of Analytical Science (Third Edition)*, P. Worsfold, C. Poole, A. Townshend, and M. Miró, Eds. Oxford: Academic Press, 2019, pp. 154-160.

[36] Yunus, Jonas, and Lakard, "Potentiometric Biosensors," in *Encyclopedia of Biophysics*, G. C. K. Roberts, Ed. Berlin, Heidelberg: Springer Berlin Heidelberg, 2013, pp. 1941-1946.

[37] Walker, Roshkolaeva, Chapoval, and Dick, (2021) "Recent Advances in Potentiometric Biosensing," (in eng), *Curr Opin Electrochem.* 28:10.1016/j.coelec.2021.100735vol. p.^pp. Aug.

[38] Malhotra and Ali, "Chapter 1 - Nanomaterials in Biosensors: Fundamentals and Applications," in *Nanomaterials for Biosensors*, B. D. Malhotra and M. A. Ali, Eds.: William Andrew Publishing, 2018, pp. 1-74.

[39] Sadeghi, "Amperometric Biosensors," in *Encyclopedia of Biophysics*, G. C. K. Roberts, Ed. Berlin, Heidelberg: Springer Berlin Heidelberg, 2013, pp. 61-67.

[40] Dzyadevych and Jaffrezic-Renault, "6 - Conductometric biosensors," in *Biological Identification*, R. P. Schaudies, Ed.: Woodhead Publishing, 2014, pp. 153-193.

[41] Jaffrezic-Renault and Dzyadevych, (2008) "Conductometric Microbiosensors for Environmental Monitoring," (in eng), *Sensors (Basel).* 8:2569-2588. 10.3390/s8042569vol. no. 4, p.^pp. Apr 11.

[42] Dzyadevych and Jaffrezic-Renault, "Conductometric biosensors," 2014, pp. 153-193.

[43] Damborský, Švitel, and Katrlík, (2016) "Optical biosensors," (in eng), *Essays Biochem.* 60:91-100. 10.1042/ebc20150010vol. no. 1, p.^pp. Jun 30.

[44] Singh, "Surface Plasmon Resonance: A Boon for Viral Diagnostics," in *Reference Module in Life Sciences*: Elsevier, 2017.

[45] Chen *et al.*, "Review of Integrated Optical Biosensors for Point-of-Care Applications," *Biosensors*, vol. 10, no. 12. doi: 10.3390/bios10120209

[46] Vanengelenburg and Palmer, (2008) "Fluorescent biosensors of protein function," *Current Opinion in Chemical Biology.* 12:60-65. https://doi.org/10.1016/j.cbpa.2008.01.020vol. no. 1, p.^pp. 2008/02/01/.

[47] Piliarik, Vaisocherová, and Homola, (2009) "Surface plasmon resonance biosensing," (in eng), *Methods Mol Biol.* 503:65-88. 10.1007/978-1-60327-567-5_5vol. p.^pp.

[48] Vakilian and Majlis, "Study of interdigitated electrode sensor for lab-on-chip applications," in *2014 IEEE International Conference on Semiconductor Electronics (ICSE2014)*, 2014, pp. 201-204.

[49] Igreja and Dias, (2006) "Dielectric response of interdigital chemocapacitors: The role of the sensitive layer thickness," *Sensors and Actuators B: Chemical.* 115:69-78. https://doi.org/10.1016/j.snb.2005.08.019vol. no. 1, p.^pp. 2006/05/23/.

[50] Ibrahim, Claudel, Kourtiche, Nadi, Montaigne, and Lengaigne, "Optimization of planar interdigitated electrode array for bioimpedance spectroscopy restriction of the number of electrodes," in *2011 Fifth International Conference on Sensing Technology*, 2011, pp. 612-616: IEEE.

[51] Geng *et al.*, (2008) "Self-assembled monolayers-based immunosensor for detection of Escherichia coli using electrochemical impedance spectroscopy," 53:4663-4668. vol. no. 14, p.^pp.

[52] Kim, Kim, Kim, Jung, Jeon, and Lee, (2023) "Sustainable and environmentally viable perovskite solar cells," *EcoMat.* n/a:e12319. https://doi.org/10.1002/eom2.12319https://doi.org/10.1002/eom2.12319 vol. no. n/a, p.^pp. 2023/01/11.

[53] Zhang, Li, Sun, Wang, Wang, and Jen, (2021) "Design of Superhydrophobic Surfaces for Stable Perovskite Solar Cells with Reducing Lead Leakage," *Advanced Energy Materials.* 11:2102281. https://doi.org/10.1002/aenm.202102281https://doi.org/10.1002/aenm.202102281 vol. no. 41, p.^pp. 2021/11/01.

[54] Chen *et al.*, (2020) "SERS imaging-based aptasensor for ultrasensitive and reproducible detection of influenza virus A," *Biosensors and Bioelectronics.* 167:112496. https://doi.org/10.1016/j.bios.2020.112496vol. p.^pp. 2020/11/01/.

[55] Zhu *et al.*, (2011) "Robust superhydrophobic surfaces with mechanical durability and easy repairability," *Journal of Materials Chemistry.* 21:15793-15797. 10.1039/C1JM12513C10.1039/C1JM12513C vol. no. 39, p.^pp.

[56] Patois *et al.*, (2010) "Microtribological and corrosion behaviors of 1H,1H,2H,2H-perfluorodecanethiol self-assembled films on copper surfaces," *Surface and Coatings Technology.* 205:2511-2517. https://doi.org/10.1016/j.surfcoat.2010.09.052vol. no. 7, p.^pp. 2010/12/25/.

[57] Tian, Liu, and Deng, (2006) "Electrochemical Growth of Gold Pyramidal Nanostructures: Toward Super-Amphiphobic Surfaces," *Chemistry of Materials.* 18:5820-5822. 10.1021/cm062383rvol. no. 25, p.^pp. 2006/12/01.

[58] Zhou, Jimmy Huang, Ding, and Liu, (2014) "Aptamer-based biosensors for biomedical diagnostics," *Analyst.* 139:2627-2640. 10.1039/C4AN00132J10.1039/C4AN00132J vol. no. 11, p.^pp.

[59] Han, Liang, and Zhou, "Design Strategies for Aptamer-Based Biosensors," *Sensors*, vol. 10, no. 5, pp. 4541-4557. doi: 10.3390/s100504541

[60] Justiz Vaillant, Jamal, Patel, and Ramphul, "Immunoglobulin," in *StatPearls*Treasure Island (FL): StatPearls Publishing

[61] Dietzen, "13 - Amino Acids, Peptides, and Proteins," in *Principles and Applications of Molecular Diagnostics*, N. Rifai, A. R. Horvath, and C. T. Wittwer, Eds.: Elsevier, 2018, pp. 345-380.

[62] Azam, Bukhari, Liaqat, and Miran, "Emerging Methods in Biosensing of Immunoglobin G—A Review," *Sensors*, vol. 23, no. 2. doi: 10.3390/s23020676

[63] Vidarsson, Dekkers, and Rispens, (2014) "IgG Subclasses and Allotypes: From Structure to Effector Functions," (in English), 5:10.3389/fimmu.2014.00520Review vol. p.^pp. 2014-October-20.

[64] Schroeder and Cavacini, (2010) "Structure and function of immunoglobulins," *Journal of Allergy and Clinical Immunology.* 125:S41-S52. https://doi.org/10.1016/j.jaci.2009.09.046vol. no. 2, Supplement 2, p.^pp. 2010/02/01/.

[65] Azam, Bukhari, Liaqat, and Miran, (2023) "Emerging Methods in Biosensing of Immunoglobin G—A Review," 23:676. vol. no. 2, p.^pp.

[66] Liang, Hou, Tang, Sun, and Luo, (2021) "An advanced molecularly imprinted electrochemical sensor for the highly sensitive and selective detection and determination of Human IgG," 137:107671. vol. p.^pp.

[67] Zarei, Ghourchian, Eskandari, and Zeinali, (2012) "Magnetic nanocomposite of anti-human IgG/COOH–multiwalled carbon nanotubes/Fe3O4 as a platform for electrochemical immunoassay," 421:446-453. vol. no. 2, p.^pp.

[68] Chen, Song, Han, Li, Luo, and Bioelectronics, (2021) "Low fouling electrochemical biosensors based on designed Y-shaped peptides with antifouling and recognizing branches for the detection of IgG in human serum," 178:113016. vol. p.^pp.

[69] Liu *et al.*, (2021) "Ultrafast, sensitive, and portable detection of COVID-19 IgG using flexible organic electrochemical transistors," 7:eabg8387. vol. no. 38, p.^pp.

[70] Yuan, Giovanni, Xie, Fan, and Leong, (2014) "Ultrasensitive IgG quantification using DNA nano-pyramids," 6:e112-e112. vol. no. 7, p.^pp.

[71] Barman *et al.*, (2020) "A polyallylamine anchored amine-rich laser-ablated graphene platform for facile and highly selective electrochemical IgG biomarker detection," 30:1907297. vol. no. 14, p.^pp.

[72] Medhi, Baruah, Singh, Betty, and Mohanta, (2022) "Au nanoparticle modified GO/PEDOT-PSS based immunosensor probes for sensitive and selective detection of serum immunoglobulin g (IgG)," 575:151775. vol. p.^pp.

[73] Raja, Vedhanayagam, Preeth, Kim, Lee, and Han, (2021) "Development of two-dimensional nanomaterials based electrochemical biosensors on enhancing the analysis of food toxicants," 22:3277. vol. no. 6, p.^pp.

[74] Bai *et al.*, (2021) "Preparation of IgG imprinted polymers by metal-free visible-light-induced ATRP and its application in biosensor," 226:122160. vol. p.^pp.

[75] Hashemi *et al.*, (2021) "Ultra-precise label-free nanosensor based on integrated graphene with Au nanostars toward direct detection of IgG antibodies of SARS-CoV-2 in blood," 894:115341. vol. p.^pp.

[76] Patella *et al.*, (2022) "Electrochemical Synthesis of Zinc Oxide Nanostructures on Flexible Substrate and Application as an Electrochemical Immunoglobulin-G Immunosensor," 15:713. vol. no. 3, p.^pp.

[77] Park *et al.*, (2019) "Self-assembly of nanoparticle-spiked pillar arrays for plasmonic biosensing," 29:1904257. vol. no. 43, p.^pp.

[78] Vezza *et al.*, (2021) "An electrochemical SARS-CoV-2 biosensor inspired by glucose test strip manufacturing processes," 57:3704-3707. vol. no. 30, p.^pp.

[79] Solin, Orelma, Borghei, Vuoriluoto, Koivunen, and Rojas, (2019) "Two-Dimensional Antifouling Fluidic Channels on Nanopapers for Biosensing," *Biomacromolecules.* 20:1036-1044. 10.1021/acs.biomac.8b01656vol. no. 2, p.^pp. 2019/02/11.

[80] Sun, Aguila, Perman, Butts, Xiao, and Ma, (2018) "Integrating Superwettability within Covalent Organic Frameworks for Functional Coating," *Chem.* 4:1726-1739. https://doi.org/10.1016/j.chempr.2018.05.020vol. no. 7, p.^pp. 2018/07/12/.

[81] Chung *et al.*, (2012) "Silver-perfluorodecanethiolate complexes having superhydrophobic, antifouling, antibacterial properties," 366:64-69. vol. no. 1, p.^pp.

[82] Tuerk and Gold, (1990) "Systematic evolution of ligands by exponential enrichment: RNA ligands to bacteriophage T4 DNA polymerase," (in eng), *Science.* 249:505-10. 10.1126/science.2200121vol. no. 4968, p.^pp. Aug 3.

[83] Ellington and Szostak, (1990) "In vitro selection of RNA molecules that bind specific ligands," (in eng), *Nature.* 346:818-22. 10.1038/346818a0vol. no. 6287, p.^pp. Aug 30.

[84] Robertson and Joyce, (1990) "Selection in vitro of an RNA enzyme that specifically cleaves single-stranded DNA," (in eng), *Nature.* 344:467-8. 10.1038/344467a0vol. no. 6265, p.^pp. Mar 29.

[85] Ouellet, Foley, Conway, and Haynes, (2015) "Hi-Fi SELEX: A High-Fidelity Digital-PCR Based Therapeutic Aptamer Discovery Platform," (in eng), *Biotechnol Bioeng.* 112:1506-22. 10.1002/bit.25581vol. no. 8, p.^pp. Aug.

[86] Wu *et al.*, (2014) "Recent trends in SELEX technique and its application to food safety monitoring," (in eng), *Mikrochim Acta.* 181:479-491. 10.1007/s00604-013-1156-7vol. no. 5-6, p.^pp. Apr.

[87] Darmostuk, Rimpelova, Gbelcova, and Ruml, (2015) "Current approaches in SELEX: An update to aptamer selection technology," (in eng), *Biotechnol Adv.* 33:1141-61. 10.1016/j.biotechadv.2015.02.008vol. no. 6 Pt 2, p.^pp. Nov 1.

[88] Abedalwafa *et al.*, (2020) "An aptasensor strip-based colorimetric determination method for kanamycin using cellulose acetate nanofibers decorated DNA-gold nanoparticle bioconjugates," (in eng), *Mikrochim Acta.* 187:360. 10.1007/s00604-020-04348-xvol. no. 6, p.^pp. May 29.

[89] Sharma, Bhardwaj, and Jang, (2020) "Label-Free, Highly Sensitive Electrochemical Aptasensors Using Polymer-Modified Reduced Graphene Oxide for Cardiac Biomarker Detection," (in eng), *ACS Omega.* 5:3924-3931. 10.1021/acsomega.9b03368vol. no. 8, p.^pp. Mar 3.

[90] Yao, Wang, Wang, Wang, and Li, (2019) "Development of a chemiluminescent aptasensor for ultrasensitive and selective detection of aflatoxin B1 in peanut and milk," (in eng), *Talanta.* 201:52-57. 10.1016/j.talanta.2019.03.109vol. p.^pp. Aug 15.

[91] Kukushkin *et al.*, (2019) "Highly sensitive detection of influenza virus with SERS aptasensor," (in eng), *PLoS One.* 14:e0216247. 10.1371/journal.pone.0216247vol. no. 4, p.^pp.

[92] Sadeghi *et al.*, (2018) "Optical and electrochemical aptasensors for the detection of amphenicols," *Biosensors and Bioelectronics.* 118:137-152. https://doi.org/10.1016/j.bios.2018.07.045vol. p.^pp. 2018/10/30/.

[93] Pashazadeh, Mokhtarzadeh, Hasanzadeh, Hejazi, Hashemi, and De La Guardia, (2017) "Nano-materials for use in sensing of salmonella infections: Recent advances," *Biosensors and Bioelectronics.* 87:1050-1064. https://doi.org/10.1016/j.bios.2016.08.012vol. p.^pp. 2017/01/15/.

[94] Zahra, Khan, and Luo, (2021) "Advances in Optical Aptasensors for Early Detection and Diagnosis of Various Cancer Types," (in English), 11:10.3389/fonc.2021.632165Mini Review vol. p.^pp. 2021-February-25.

[95] Yi *et al.*, (2020) "The research of aptamer biosensor technologies for detection of microorganism," *Applied Microbiology and Biotechnology.* 104:9877-9890. 10.1007/s00253-020-10940-1vol. no. 23, p.^pp. 2020/12/01.

[96] Zou, Wu, Gu, Shen, and Mao, (2019) "Application of Aptamers in Virus Detection and Antiviral Therapy," (in English), 10:10.3389/fmicb.2019.01462Review vol. p.^pp. 2019-July-03.

[97] Zhuo *et al.*, (2017) "Recent Advances in SELEX Technology and Aptamer Applications in Biomedicine," 18:2142. vol. no. 10, p.^pp.

[98] Heo *et al.*, (2016) "An aptamer-antibody complex (oligobody) as a novel delivery platform for targeted cancer therapies," *Journal of Controlled Release.* 229:1-9. https://doi.org/10.1016/j.jconrel.2016.03.006vol. p.^pp. 2016/05/10/.

[99] Lee, Lee, Kim, Noh, Noh, and Lee, (2015) "Pharmacokinetics of a Cholesterol-conjugated Aptamer Against the Hepatitis C Virus (HCV) NS5B

Protein," *Molecular Therapy - Nucleic Acids.* 4:10.1038/mtna.2015.30vol. p.^pp.

[100] Gan *et al.*, (2022) "Advances in Aptamer-Based Biosensors and Cell-Internalizing SELEX Technology for Diagnostic and Therapeutic Application," 12:922. vol. no. 11, p.^pp.

[101] Jiang, Zhao, Li, Li, and Huang, (2021) "2D MOF-Based Photoelectrochemical Aptasensor for SARS-CoV-2 Spike Glycoprotein Detection," *ACS Applied Materials & Interfaces.* 13:49754-49761. 10.1021/acsami.1c17574vol. no. 42, p.^pp. 2021/10/27.

[102] Tran *et al.*, (2011) "Nanocrystalline diamond impedimetric aptasensor for the label-free detection of human IgE," *Biosensors and Bioelectronics.* 26:2987-2993. https://doi.org/10.1016/j.bios.2010.11.053vol. no. 6, p.^pp. 2011/02/15/.

[103] Chang, Tang, Wang, Jiang, and Li, (2010) "Graphene Fluorescence Resonance Energy Transfer Aptasensor for the Thrombin Detection," *Analytical Chemistry.* 82:2341-2346. 10.1021/ac9025384vol. no. 6, p.^pp. 2010/03/15.

[104] Cheng *et al.*, (2020) "A sensitive homogenous aptasensor based on tetraferrocene labeling for thrombin detection," *Analytica Chimica Acta.* 1111:1-7. https://doi.org/10.1016/j.aca.2020.03.017vol. p.^pp. 2020/05/15/.

[105] Fan, Zhu, Wu, Zhang, Wang, and Wen, (2022) "A flexible label-free electrochemical aptasensor based on target-induced conjunction of two split aptamers and enzyme amplification," *Sensors and Actuators B: Chemical.* 363:131766. https://doi.org/10.1016/j.snb.2022.131766vol. p.^pp. 2022/07/15/.

[106] Wang, Veselinovic, Yang, Geiss, Dandy, and Chen, (2017) "A sensitive DNA capacitive biosensor using interdigitated electrodes," *Biosensors and Bioelectronics.* 87:646-653. https://doi.org/10.1016/j.bios.2016.09.006vol. p.^pp. 2017/01/15/.

[107] Aspermair *et al.*, (2021) "Reduced graphene oxide–based field effect transistors for the detection of E7 protein of human papillomavirus in saliva," *Analytical and Bioanalytical Chemistry.* 413:779-787. 10.1007/s00216-020-02879-zvol. no. 3, p.^pp. 2021/01/01.

[108] Fenoy, Von Bilderling, Knoll, Azzaroni, and Marmisollé, (2021) "PEDOT: Tosylate-Polyamine-Based Organic Electrochemical Transistors for High-Performance Bioelectronics," 7:2100059. vol. no. 6, p.^pp.

[109] Vezza *et al.*, *An uncomplicated electrochemical sensor combining a perfluorocarbon SAM and ACE2 as the bio-recognition element to sensitively and specifically detect SARS-CoV-2 in complex samples*. 2020.

[110] Ding *et al.*, (2017) "Rapid and label-free detection of interferon gamma via an electrochemical aptasensor comprising a ternary surface monolayer on a gold interdigitated electrode array," 2:210-217. vol. no. 2, p.^pp.

[111] Du *et al.*, (2018) "Improving the compatibility of diketopyrrolopyrrole semiconducting polymers for biological interfacing by lysine attachment," 30:6164-6172. vol. no. 17, p.^pp.

[112] Mishyn *et al.*, (2022) "Electrochemical and electronic detection of biomarkers in serum: a systematic comparison using aptamer-functionalized surfaces," 1-9. vol. p.^pp.

[113] Patois *et al.*, (2010) "Microtribological and corrosion behaviors of 1H, 1H, 2H, 2H-perfluorodecanethiol self-assembled films on copper surfaces," 205:2511-2517. vol. no. 7, p.^pp.

[114] Hasegawa, Savory, Abe, and Ikebukuro, (2016) "Methods for Improving Aptamer Binding Affinity," (in eng), *Molecules.* 21:421. 10.3390/molecules21040421vol. no. 4, p.^pp. Mar 28.